



TALLINNA TEHNIKAÜLIKOOL
TALLINN UNIVERSITY OF TECHNOLOGY

School of Engineering: Department of Civil
Engineering and Architecture: Structural Engineering
Research Group

**Determination of parameters for the design model
for timber I-joists in fire**

Parameetrite määramine puidust I-talade
tulepüsivuse arvutusmudeli jaoks

MASTER THESIS

Student: Xavier Jerez Ribas

Student code:

Supervisor: Alar Just, Professor
Katrin Nele Mäger, Early Stage
Researcher

Tallinn, 2018

(On the reverse side of title page)

AUTHOR'S DECLARATION

Hereby I declare, that I have written this thesis independently.

No academic degree has been applied for based on this material. All works, major viewpoints and data of the other authors used in this thesis have been referenced.

"19" May 2019

Author: Xavier Jerez Ribas

/signature /

Thesis is in accordance with terms and requirements

"....." 201....

Supervisor:

/signature/

Accepted for defence

"....."201... .

Chairman of theses defence commission:

/name and signature/

THESIS TASK

Student: Xavier Jerez Ribas (name, student code)

Study programme, Master Thesis Spring Erasmus EE Tallinn 04(code and title)

main speciality: Industrial Engineering Construction and Structures

Supervisor(s): Alar Just, Professor

Katrin Nele Mäger, Researcher

Thesis topic:

(in English) Determination of parameters for the design model for timber I-joists in fire

(in Estonian) Parameetrite määramine puidust I-talade tulepüsivuse arvutusmodeli jaoks

Thesis main objectives:

1. To determine parameters influencing charring of the flanges of wooden I-joists on the basis of thermal simulation results

Thesis tasks and time schedule:

No	Task description	Deadline
1.	Literature survey	April 1st
2.	Analysis of results of thermal simulations	May 1st
3.	Determination of parameters for the equations of charring	May 17th

Language: English **Deadline for submission of thesis:** "20" May 2019a

Student: "....."201....a
/signature/

Supervisor: Prof. Alar Just
"....."201....a
/signature/

Consultant: "....."201....a
/signature/

Terms of thesis closed defence and/or restricted access conditions to be formulated on the reverse side

CONTENTS

1 PREFACE	5
2 INTRODUCTION	6
2.1 History of timber structures	6
2.2 Actuality in timber structures.....	7
2.3 History of fires in timber structures	10
3 ACTION OF FIRE AND EFFECTS IN THE TIMBER STRUCTURES	12
3.1 Timber combustion and fire study	12
3.2 Factors that influence the combustion of wood	14
3.3 Timber structures	15
3.3.1 Heavy structures	15
3.3.2 Light structures	16
3.4 Resistance to fire and ways to improve it	16
4 CHARRING OF TIMBER.....	17
4.1 Actual Calculations for resistance of timber structures under the fire effects	17
4.2 Charring of timber in small cross-sections	19
4.3 One dimensional charring	19
4.4 Two-dimensional charring	21
4.5 Effect of protection on small-sized timber frame members	23
4.5.1 Protection Levels (Tiso 2018)	26
5 I-JOIST	30
5.1 General	30
5.2 I-joist Parameters Definition	32
6 DETERMINATION OF $K_{3,1}$ EQUATION.....	35
6.1 Thermal Simulation	35
6.2 Matlab Algorithm	37
6.2.1 Matlab Flowchart	37
6.2.2 Flow chart explanation.....	39
6.2.3 Results obtained by Matlab	40
6.3 Excel Analysis.....	42
6.3.1 Problem solution for first values.....	44
6.3.2 Graph.....	46
6.3.3 General Equations and Graphs	52

6.4 $k_{3,1}$ Formula	57
6.4.1 Parameter M	57
6.4.2 Parameter N	60
6.4.3 Final equation.....	62
7 RESULTS AND ANALYSIS	64
8 REAL TESTS COMPARISONS	70
8.1 Comparisons	72
9 CONCLUSIONS	74
9.1 Safir Imprecisions	74
9.2 General Equation differences	75
10 SUMMARY	77
10.1 English Summary	77
10.2 Resum en català	79
11 LIST OF REFERENCES.....	81
12 Appendix A : Calculations for the equation	83
12.1 Parameter M.....	83
13 Acknowledgments.....	88

1 PREFACE

THE STUDY OF 'DETERMINATION OF PARAMETERS FOR THE DESIGN MODEL FOR TIMBER I-JOISTS IN FIRE' SHOW THE METHODOLOGY FOR SEARCHING COEFFICIENTS ABOUT HOW TO CONSIDER AND DEFINE THE EFFECT OF FIRE ON TIMBER STRUCTURES. THIS STUDY IS A PART OF THE THESIS MADE IN TALTECH UNIVERSITY BY KATRIN NELE MAGER AND WITH THE SUPERVISION OF THE PROFESSOR ALAR JUST. IN THIS STUDY CONSISTS IN THE RESEARCH OF THE COEFFICIENT $K_{3,1}$ FORMULA, COEFFICIENT THAT DEFINES THE CHARRING ALONG THE FIRE-EXPOSED SIDE TAKING INTO ACCOUNT THE PROTECTION OFFERED BY THE INSULATION AND THE PROTECTION BOARD IN POST-PROTECTION PHASE.

INITIALLY THE SIMULATIONS ARE DONE WITH THE SAFIR PROGRAM OF SOME SPECIFIC CASES OF TIMBER STRUCTURES UNDER THE EFFECTS OF FIRE, FROM WHERE MANY DATA ARE OBTAINED. THEN THE ITERATIONS ARE MADE WITH AN ALGORITHM IN THE MATLAB PROGRAM WHERE A LOT OF RESULTS OF ALL IMPORTANT AND POSSIBLE SITUATIONS ARE OBTAINED. IN THIS PART IS WANTED TO COVER ALL THE POSSIBILITIES TO GETTING A PATRON ABOUT HOW THE FIRE AFFECTS AN I-JOIST IN CASE OF FIRE IN THE BUILDING. ONCE IT HAS THE TRANSCENDENTAL DATA, IT IS GATHERED THEM IN EXCEL SO CERTAIN BEHAVIOR PATTERNS CAN BE DEDUCTED. FROM THERE IT IS MISSING TO DEEPLY INVESTIGATE THE DATA TO SEEK TRENDS AND ARRIVE TO A FORMULA THAT REPRESENTS THEM ALL IN EXACTLY MANNER A MORE OR LESS.

AS A FINAL RESULT THE COEFFICIENT $K_{3,1}$ IS DEFINED WITH A FORMULA THAT USES VARIABLES EASIER TO OBTAIN.

ON THE OTHER HAND, SOME FIRE TESTS ARE DONE IN REAL I-JOIST TO HAVE THE SAME RESULTS. THE MAIN OBJECTIVE IS TO COMPARE THOSE RESULTS TO THE FORMULA RESULTS. THEN WITH THE COMPARATIONS IT IS POSSIBLE TO MAKE AN IDEA OF HOW THE EQUATION IS FITTED TO REALITY.

FINALLY THE COMPARISON GIVES SOME CONCLUSIONS CAN HELP TO UNDERSTAND BETTER HOW TIMBER EVOLVES AGAINST FIRE AND WHICH ASPECTS ARE MISSING TO IMPROVE THE BEHAVIOR OF WOOD IN CASE OF FIRE.

2 INTRODUCTION

2.1 History of timber structures

Timber nowadays and during lots of years has been one of the most used materials in the construction world. During the Neolithic to the Industrial Revolution it was the first material used for a majority of things, because was a very abundant material, it was easy to work with it. Probably the first homes and places to protect the cold were made of timber, after the men left the caves to live.

When the Industrial Revolution starts, the concrete and steel becomes the new and the most used materials in the construction. The houses and mostly the big structures started being made by these materials and the timber stayed on a second plane. The reinforced concrete and steel, which due to its simplicity of series manufacture and the ability to cover larger lights, were progressively determined as predominant structural materials in the 20th century, relegating the use of timber to smaller constructions. But the history of the timber in construction didn't finish there.

In recent decades there has been a rediscovery of timber, especially in industrialized countries, where contemporary consciousness advocates the need to protect natural resources. The large amounts of energy and the high emissions of greenhouse gases, necessities to produce high-tech construction materials such as steel, concrete or aluminium, are incompatible with this growing concept of environmental sustainability. In this sense, wood constitutes the support structure of the tree and has the advantage of being a structural product in origin, without the need for an industrial transformation process associated with the high energy cost that this entails. The use of wood as a construction material also provides great ecological benefits. The timber elements placed on site fix the carbon captured in their cell walls during the entire life of the structure, contributing to a fully sustainable development. With the evolution of technology and construction methods and systems have been discovered to form more resistant structures with materials not as tenacious as steel or reinforced concrete. This has allowed timber to re-enter the scene as it is now allowed to form larger, more durable structures of better quality. [1]

In recent years, the continued evolution of the electronics and computer sectors has allowed the appearance on the market of a wide variety of computer programs of specific design that process and transmits information in the factory to high precision numerical control machines. The stages of the production process of design, machining and assembly of the timber structure is now possible to perform in facilities that may be far from the final interlocking of the same. By means of this system of execution, production yields are increased and possible deterioration in materials collected on site, excessive assembly times or execution errors by unqualified personnel is avoided. The timber structure is simply transported, whole or in parts, from the factory to the work site and placed as one more piece of the complete structure. Unions and the beams are the points of transmission of stress between the elements of a structure being its design and calculation in which there is generally less emphasis and, however, have greater importance and complexity because they are the cause of numerous structural damage. The cost of the beams and joints in the overall calculation of a timber construction (including its design, manufacture and assembly) is around 50-60%, which makes its optimization a very important aspect to be taken into account by architects and engineers for the future viability of the project. Currently, traditional beams and unions have a very high level of execution, faster assembly, visual finish highly valued by users, economy of materials and provide very good resistance to fire. In the last years it has been wanted to replace these traditional structures with modern ones.

The topic that is studied in this thesis is the beams, which are the parts that hold all the top plane elements of the building in structural terms. In our case, we look at the work that the beams of these structures make and a thorough study of the modification of their properties during fire action to find solutions. Especially here the I-joists are studied, which is a modern beam designed for having a lot of resistance against the heavy charges and the fire effects, it is explained later.

[2][3]

2.2 Actuality in timber structures

For all the reasons that are said in the last chapter, nowadays in the world the 18% of the population are living in houses made of timber, that are almost 1300 million of people. This happens especially in the less developed countries according with the information of FAO (United Nations Organization for Food and Agriculture). Even so there are lots of timber structures in developed countries like EUA, UK, the Baltic countries, etc, normally for comfort and cultural

reasons (In EUA for example the idea of living all life in one house is not common in many zones, so the solution is building cheap houses made of timber). [4]

This is because the timber structures have lots of advantages against the traditional concrete and brick structures, all thanks to the development, modernization and technical improvements in this sector. In the present it has been raised the point that the timber structures can give the option of build one construction in 4 or 5 months. There are exceptional cases where the construction has been made in 5 days, thing that is awesome. Another positive aspect is the possibility of being built progressively either for lack of budget or because new needs arise.

Even though it may not seem like the wood has a great mechanical resistance, its lightness does not prevent it from being a solid material, capable of offering the same protection as walls built with bricks. Let's not forget that timber structures are common in houses built in the traditional way, and that the choice of this material obeys its enormous strength. To its solidity it is added a great durability, much greater than one tends to believe. They resist well the wear produced by humidity, wind and the sun and, in short, their durability is practically eternal.

Apart of the structural benefits, living in a timber house gives to the residents the feeling of comfort and well-being. In fact, wood is a hygroscopic material. In practice, this translates into a greater ability to regulate indoor air humidity, which, together with its insulating power, provides a pleasant feeling of well-being. When it comes to achieving energy efficiency, in fact, wood is an interesting material to thermally insulate the house and save on the electricity bill or the use of firewood to keep it warm in winter and cool in summer. It's possible to enhance its thermal insulation if it is resorted to supplementary insulators that also help to isolate it acoustically, although wood itself is a good insulator against acoustic pollution, an interesting property also usable inside the home. Wood is a renewable material that, controlled by a sustainable production, turns it into an ecological option. In addition, compared to the usual building materials and the construction process, it saves money.

In addition, with the proper treatment of the wood, they do not represent a greater risk than the classic houses in case of fire. On the contrary, wood is a fire-stable material, which is consumed very slowly when flames attack it, not like some materials used in the current architecture that are much more flammable and are consumed faster. Thanks to treatments with fire-retardant substances, combustion is not faster than that of a building made of cement, bricks and concrete.

In this aspect, there is also a great ignorance, because in general people don't have the correct information.

All these advantages have allowed society and companies to design and build ever larger and more complex buildings and more regularly. So more and more material is used with what leads to more complex structures and more complicated facilities. The *Picture 1* shows the Mjostarnet which is the largest building made by timber in the world.



Picture 1 : Ecohabitar (2018) Timber Structure, photo by www.ecohabitar.org

The bigger the building is, more people are working or living in there and the security must be more efficient. That is why the investment in fire safety and prevention is a vital and necessary part of the construction business with timber to survive and props efficiently and firmly. For all that has been said, the way how these instructions are carried out and the security measures that are applied in them has to take into account very carefully. Therefore, an in-depth study has been carried out on how to define certain parameters to predict the behaviour of these structures in case of fire and how to prevent the quickly collapse of the building. [5][6]

2.3 History of fires in timber structures

The creation of fire by the scratching of two sticks and their use as fuel for the cooking and heating has decisively influenced the distrust of wood as structural element. The historical development of large fires and the deaths committed in cities with timber buildings has increased that distrust.

Among them we can mention those of Rome, in the year 64, the one in London of 1666 (that gave rise to the first norm against the timber for incorporate barriers between mediating buildings), where all the houses were made by timber and the 87,5% of the buildings were destroyed during this fire. In England the buildings made of brick started being made after this event and the timber decreases his activity in construction. And on the other hand the fire of Trondheim (Norway) of 1717 which have influenced the collective opinion of later generations around the world about the timber structures.

Through the Industrial Revolution in the 18th century and in USA in the 19th century, fires continued, despite the fact that it began to prohibit the construction with timber structure and its replacement by masonry, concrete, bricks and steel. Public departments were formed against fires, public water supplies were installed with groundwater pipelines and fire hydrants, and there was an improvement of fire trucks. The use of steel and concrete in structures (assuming that have more resistance against the fire) was taken as the solution against this problem, falsehood that came to demonstrate other great fires like those Chicago 1871 and San Francisco 1906, which had nothing to do with wood and caused same ravages. [7]

Points to highlight from these historical experiences that favour the use of wood for construction:

- The fires begin and develop due to causes external to the structure but the end destroying the building.
- Very few buildings that suffer a fire can take advantage of its structure later since the high temperatures reached in a fully developed fire they profoundly modify the internal structure of the materials, be it steel, concrete, brick or timber. Or at least the doubt remains and they end up falling under the pickaxe.

- In a poorly developed fire, the structure may be maintained, but in steel it is very low and reinforced concrete somewhat larger.
- Statistics show that buildings with timber structures burn as much as those of steel or concrete structure with the difference that the structure does contribute as fuel to the fire and can harm in its expansion.

The experience accumulated in this type of fire led to the town councils and the central governments to establish legislative measures that minimize the effects of same. These norms have been homogenized in the different countries, reaching establish the basic criteria that are basically reduced to giving up the structure and the building and demand a minimum resistance that allows the evacuation of people and the intervention of fire fighters. One of the first measures was the prohibition of combustible such as wood as a structural element. This measure, logically it did not solve the problem. So as they realized that the wood was not to blame for the serious fires that occurred, it began to recover the confidence in the use of this material and the wooden constructions were resumed. [1]

3 ACTION OF FIRE AND EFFECTS IN THE TIMBER STRUCTURES

3.1 Timber combustion and fire study

Timber burns through chemical reaction (combustion) from outside to inside decreasing gradually its section proportionally to its exposure to fire. In the combustion of the wood its volume is fundamental: thin pieces burn with ease while thick ones are more resistant, for that reason heavy structures views can be left, while light ones are covered with non-combustible materials called insulators.

The study of the phenomenon of fires has led to the development of some concepts which are basic and common to the regulations and codes. These concepts make references to individual materials (reaction to fire), to structural elements (resistance to fire) and the general definition an action of fire (conflagration). These concepts affect directly in the characteristics of a timber structure and are defined as in the following points:

- **Reaction to fire:** The reaction to fire refers to the material and evaluates how it behaves in the presence of fire. It may favour the fire or have no influence on the evolution of it. In definitive is defined if the material is combustible or not and is classified according to its degree of combustibility.
- **Fire Resistance:** Fire resistance refers to constructive or structural elements and measures the time during which said element continues to fulfil its function in the building (for example a door, a diving wall made of boards, a beam, a floor, etc.) These functions are the carrying capacity, the integrity of element (E), the insulation (I) and the closure capacity before a fire and are defined in the regulations, regulations or codes for buildings.
- **Fire or conflagration:** A fire is caused by the combustion of construction elements, furniture and decoration and it develops randomly in space and time depending on the amount and type materials that compose it. The structure of a building contributes very little in the development of fire except timber and in the final phase of the fire. The fire includes the behaviour of all materials and elements that make up the mass of the fire influencing each other in a completely random way. For it to start and develop it is necessary that there are combustible materials, oxygen (air) and a source of heat. Fire in vulgar terms chemical is the

chemical oxidation reaction of exothermic character. Inflammation is the flame formation that occurs due to the emissions of gases in contact with air. The ignition is the phenomenon that initiates combustion. It depends on the density, dimensions and shape, humidity, speed and intensity of heating, supply and air speed. In the wood is produced around 230°C, although in the simulations the carbonized wood at 300°C is considered. The following expression shows the components that permit the creation of fire.

$\text{Fire} = \text{Gas materials} + \text{Oxygen} + \text{Temperature}$

The Initial Phase of the fire begins when an excessive temperature rise initiates the combustion of a material (curtain, furniture, coating, carpet, wastepaper basket, etc). During this phase the fire can still be controlled and depends on the reaction to the fire of the materials. In the Development Phase the increase in heat released by the materials that enter into combustion and the flames gradually transmit the fire to the whole building. The reaction to fire of the materials happens then to have a secondary role, it only influences the propagation. The fire resistance of structural elements begins to play an important role, since it depends on saving human life and material goods. Complementarily from the beginning of the fire the emission of gases and fumes takes place that has a great influence on people because they can cause death by suffocation in the worst case or loss of consciousness, irritations in the eyes and difficulty of vision of the outputs at the best. The emission of gases and fumes is associated with the reaction to the fire of materials. [5]

As regards fire, it acts similarly in the explained phases when it is affecting the type of beams that are analysed in this study. This known evolution helps to better understand the coefficient it's being looked for and how to treat the data to find an expression that best defines the evolution of fire.

3.2 Factors that influence the combustion of wood

The timber has lot of physical and chemical properties which affects directly in the combustion of the material.

- Wood species: Conifers tend to have shorter charring times than hardwoods because they contain resins and natural oils that swell easily and quickly. But there are some procedures to avoid those effects by the resins and for make more resistant timbers against the effects of the fire. The wood of broadleaf pores (oak for example) because they contain more air inside that facilitates its spread.
- Density: The carbonization time is proportional to the density of the wood. The lightest woods they are the most porous and, therefore, burn faster than heavy ones because they have more air available for having the exothermic reaction.
- Squad, surface and shape: In the thick pieces the flash point is delayed because the surface to be heated is greater for the same heat source. Rough and angular surfaces favour the inflammation, because the fire finds unique entry points that burn with more easily. On smooth surfaces the flames lick the faces and take longer to penetrate inland.
- Moisture content: the more moisture the wood has, the longer it take to get the combustion since first the water contained in the wood has to be evaporated.
- Size of the heat source: The heat source must provide enough energy to het the entire piece, not enough a very intense point source.
- Coefficient of heat conductivity of wood: Its value is very low, especially in the direction perpendicular to the fibber. It is a factor key in the resistance and is superior to that of steel and concrete.

Note: Coal protects the piece of wood from the action of fire because its coefficient of Conductivity Calorific is $\frac{1}{4}$ (and can reach the $\frac{1}{6}$) of the wood. Charcoal (which is what is created in the combustion of wood) also burns at temperatures above 500°C which are more difficult to reach, although once they are reached it continues to burn without the need for

heat, as long as there is enough oxygen. The coal layer is going consuming and creating continuously and slowly since oxygen is also decreasing playing its protective role.

- **Specific Heat:** The specific heat of the wood is low, from 0,4 to 0,7 kcal/kg1C, which means that it needs a lot of heat to reach 150°C, temperature at which they begin to fall off combustible gases and therefore to appear the flames.
- **Carbon formation and carbonization speed:** In wood, unlike other materials coal is formed in the outer layers which delays the diffusion of heat into its interior which the acts as an insulator since it is more porous the wood. The inner area of the piece does not suffer hardly thermal modification and retains intact its mechanical properties, steel or concrete behave in change in a totally different way, altering its internal structure.

The approximate carbonization rate of the wood is 0,65 mm/min this means that the wood in a fire is predictable, something that does not happen with the rest of materials whose response is random, to such an extent that the carbonization rate is used in the calculation of timber structures in the fire hypothesis. It is also by the crunches before breaking. This allows planning the work of extinction and evacuation with a certain order and security, something important in a fire. [1]

3.3 Timber structures

3.3.1 Heavy structures

The structure is burning and weakening progressively and slowly due to following reasons:

- Its low thermal conductivity causes the temperature to rise only in the surface remaining the interior, more stable, thus delaying the process of combustion.
- The surface carbonization that is produced prevents, on the one hand, the release of gases and on the other penetration of heat. As in the previous case, the process of combustion when the inner part of the structural parts is protected by the carbonized surfaces layers.

- Because its thermal expansion is negligible, it does not destabilize structures and does not so. [1]

3.3.2 Light structures

The timber burns and weakens very quickly so the collapse is very fast what it obligates to protect it with external means or layer protection. This protection is not only easy but inherent in the system since the lightweight frameworks themselves must be covered with boards to complete the correct functioning of the system. That some of these boards are made of gypsum protecting the structure does not add or remove anything to the system itself. More or less this is what it's being analysed in this study. [1]

3.4 Resistance to fire and ways to improve it

A frequent error is to believe that improving the reaction to fire improves the resistance to fire. The reaction to fire only refers to the combustibility of the material and evaluates with specific test, while fire resistance is evaluated with other essays that measure the time that the element performs its function. In the case of timber structural elements the main parameter is the carbonization speed. Some of the ways to improve the fire resistance of timber structural element are:

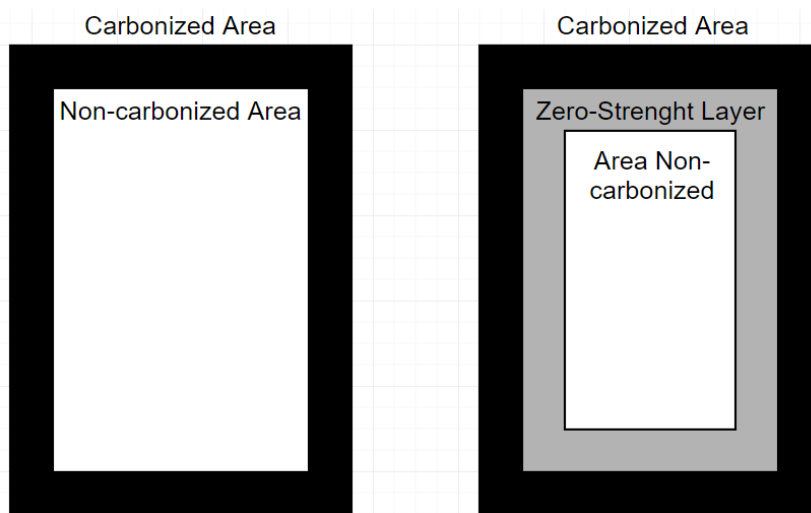
- Add a sacrificial section of timber: Depending on the time required, it size section so that once that time has elapsed the section that remains continue to play its structural role.
- Add a sacrificial section of a non-combustible material or passive protection. By gypsum boards, so that they can't increase their temperature. Gypsum does not burn and also isolates a certain time because it must also expel the water that carries.
- Add an intumescent sacrificial section that is operative, like the previous ones, for a certain time. In timber structures they are underdeveloped and they are not too reliable. [1]

In our structures some of these preventions are added to reduce the power of fire.

4 CHARRING OF TIMBER

4.1 Actual Calculations for resistance of timber structures under the fire effects

Nowadays in the world of the timber structures there are two calculation methods where it is necessary to know the charring of the timber structures. This two calculation methods are the “Reduced Properties Method” and the “Reduced Cross-Section Method”. The Picture 2 shows the two cross-sections where the important parts in each method.



Picture 2 : Reduced Properties Method Area and Reduced Cross-section Method

The "Reduced Properties Method" is based on taking the depth of carbonization, knowing which the carbonized area is and which is not. Once the area is known, the properties of resistance are modified to make an approximation of the real properties that the structure of the timber has in view of carbonisation during the fire. This reduction of the properties is carried out since the line that separates the charred area from which it is not is not clearly defined because the temperature of this zone is also very high, so it is necessary to apply changes to the mechanical properties this area since they are never fully functional.

On the other hand, the "Reduced Cross-Section Method" of the area follows guidelines similar to the previous method but in practice it is a bit different. In this case the charred area and the non-

charred area are considered, which divide the last one into two areas: the area that is not charred and the area of doubtful properties. The first area is the part of the section that is not charred and that it has in its fullness its characteristics, the second one is the area which is not charred but could be affected by the fire and the high temperatures. In this case to know the mechanical resistance of the timber structure, only the properties of the non-charred and non-affected part are taken into account. The dubious area is the reduction applied in the non-charred part, which acts like a border between the charred and the non-charred part. This is a way to apply a safety coefficient to the timber structure. In the case the timber is heated while the fire is happening, the timber has a reduction of its mechanical properties, both in resistance as in stiffness. This phenomenon occurs before the charring of the timber, it only happens with the heating of the timber. This phenomenon can be expressed with a "zero-strength layer", where there are no strengths and stiffness. The *Formula 1* express this phenomenon.

$$d_{ef} = d_{char,n} + d_0$$

Formula 1 : Zero-strength layer

Where:

- d_{ef} : effective charring depth [mm]
 $d_{char,n}$: notional design charring depth [mm]
 d_0 : zero – strength layer depth [mm]

The load condition affects directly on the depth of the zero-strength layer.

In both methods is necessary to know which is the charring depth and the charring area of the timber members in the timber structures, that's why having a sophisticated method on how to obtain the data can be very helpful. [8][9]

4.2 Charring of timber in small cross-sections

Timber structure materials suffer the charring effect made by the fire if the fire has a large duration and if they are not protected by an insulation material. For the calculation of this phenomenon it's necessary to reduce the original cross-section to the charring depth. This allows to know the resistance of timber members when the charring has started and the properties are being reduced.

There are two types of charring in the timber members:

- One dimensional charring. Where the charring is considered as a physical properties for specific species, timber with specific density, etc.
- Two-dimensional charring. Include the cross-section effects.

All the orientation of the surfaces exposed to the effect of fire has applicable rates and also the direction of the exposure of fire. There are no distinctions between the vertical and horizontal surfaces. [8]

4.3 One dimensional charring

The charring rate observed for one dimensional heat transfer under the fire exposure in a standard way of an unprotected semi-infinite timber slab without any fissure or gaps is defined as the one-dimensional charring rate β_0 . This type of charring can be applied in slabs of limited thickness or in cross-sections with a large width where the corners are far from the point of fire exposure.

The expression of the one dimensional charring depth $d_{char,0}$ is expressed as in the *Formula 2*.

$$d_{char,0} = \beta_0 \cdot t$$

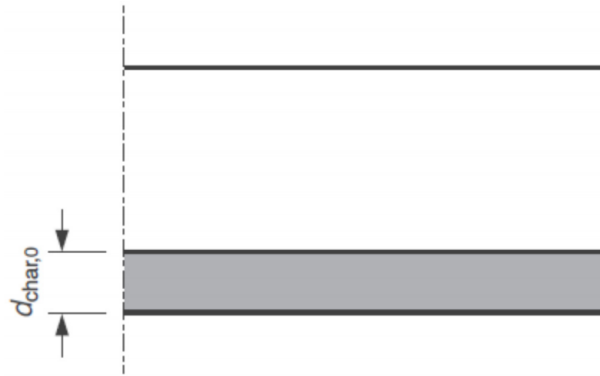
Formula 2 : Dimensional charring depth

Where:

t : time of fire exposure

β_0 : one – dimensional charring rate perpendicular to the grain

The *Picture 3* shows how the $d_{char,0}$ happens in some cases.



Picture 3 : Charring depth $d_{char,0}$

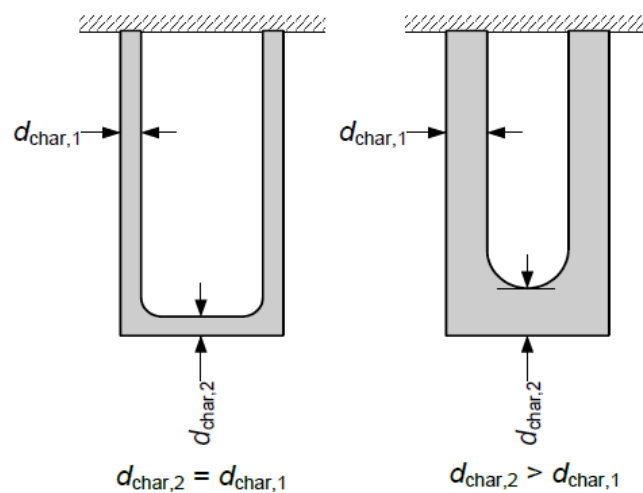
Normally the charring rate given for the softwoods is valid in Europe because these ones are used always in there. There the influence of the density in European strength classes are small and can be neglected. And its value is:

$$\beta_0 = 0,65 \text{ mm/min}$$

There are some limitations in the timber panels when they are considered under the effects of fire. The one dimensional charring rate can be used in timber-based panels where the thickness is 20 mm and the density is 450 kg/m^3 . For other thicknesses and densities some factors must be used to approximate the values more to reality. [8]

4.4 Two-dimensional charring

Once it has been spoken how the carbonization works in the flat surfaces it is need to talk about the limited surfaces, which ones are in the most common cases in fires ad which there are studied here. The rectangular cross-sections have corners, and in those corners the heat and fire flux is in two dimensional giving to the corners a rounded shape because of the charring. During the start of fire, the volume and the depth of the charring is equal in all parts of the timber member. Then, when the fire effect have had a considerable time the charring increases more in the narrow part than in the wide side as the *Picture 4* shows.

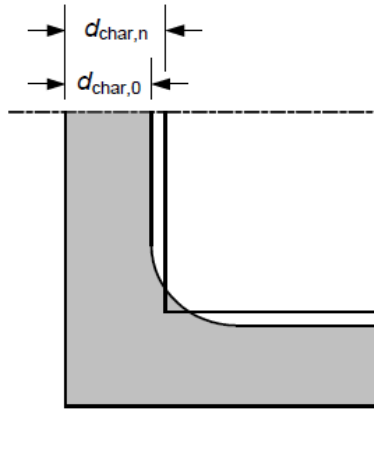


Picture 4 : Charring depth evolution

For timber members under the effects of fire in three or four sides and with normal load ratios relevant for structural design, the increase of the charring of the narrow side has a very limited effect in the resistance of timber members and can be neglected.

But in some cases the increasing of charring in narrow side must be taken into account, for example when the timber studs or joists are protected by cavity insulation on their wide sides.

For the simplicity of the calculations the residual rounded cross-section of the charring part can be replaced with a rectangular cross-section, with the objective of replacing the depth of one-dimensional charring and the rounding with an equivalent notional charring rectangular depth as the *Picture 5* shows.



Picture 5 : Equivalent notional charring depth $d_{char,n}$

As the *Formula 3* express it.

$$d_{char,0} = \beta_n \cdot t$$

Formula 3: Charring depth $d_{char,0}$

Where:

β_n : *notional charring rate*

What gives notional charring rates for timber members with rectangular cross-sections exposed to fire on three or four sides. It can vary a little depending on the material it's been used, for example:

Glued laminated timber in LVL (softwood) $\rightarrow \beta_n = 0,7 \text{ mm/min}$

Solid timber (softwood) $\rightarrow \beta_n = 0,8 \text{ mm/min}$

The charring rates take account of the fissure effects as well, and depending on the material we use different factors to simulate it. We have to consider the fissures equal or bigger than 4 mm, but we don't have any way to size that.

The *Formula 4* express the notional charring.

$$\beta_n = k_n \cdot \beta_0$$

Formula 4: Notional Charring

Where:

$$\beta_n = 0,65 \text{ mm/min}$$

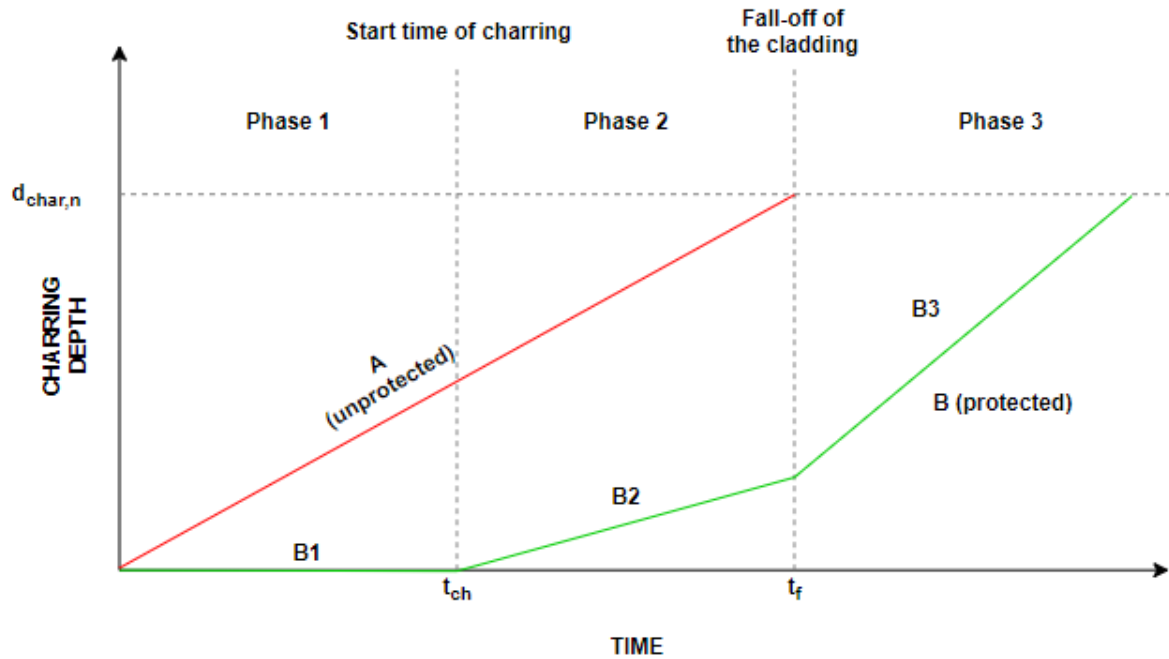
k_n : *modification factor for corner rounding*

$$k_n = 0,65 \text{ mm/min (solid timber)}$$

As a simple alternative of simplification by using notional charring depths, it's possible to consider a residual cross-section with linear and rounded boundaries. The problem is that the calculations are more complicated but it is not necessary to consider it because the difference in results is negligible. [8]

4.5 Effect of protection on small-sized timber frame members

Nowadays all the timber structures, in concrete all its parts are protected by some insulation materials before the construction of the building. And then, once they are mounted it's possible to add in the structure another type of protection like a timber board, gypsum board, etc. This protections have an important affect in case of fire and in the process of the structure while is burning, because it delays the loss of properties and resistance. In the *Graph 1* shows the evolution of a timber element during a fire in the structure.



Graph 1 : Charring phases of unprotected and initially protected timber members

Case A: In this case the structure has no protection of insulation or board and, as the *Graph 1* shows, its evolution is completely linear. The fire affects the timber and as time goes on the charring is deeper and the strength and resistance diminish in the same way.

Case B: In this case the timber structure has an insulation protection and a protection board against the fire and then the behaviour of the structure is completely different. This protection can be made by some insulation materials like gypsum, mineral wool, cellulose, etc.

For this study Case B is analysed, because our coefficient $k_{3,1}$ defines the behaviour of the timber until the fall of the board and how it evolves over time. Case B can be divided in three phases:

- *Phase 1: Encapsulation Phase*

This protection is the first which is affected for the fire and the first to be burnt. Its duration depends on the type of thickness of the applied protection added in the timber members in front of the fire point. The resistance of the board and insulation can be calculated by the sum of protection time layers preceding the timber member with the component additive method or the other possibility is declare by producers based on the test for K-classes according to EN 13501-2 (CEN,2003).

There are so many types of protection board materials and during a fire they can fall immediately when the charring has started or they can be able to stay after the charring has started behind them. The slow charring rate is defined by a protection coefficient when it starts behind the protection board s and those ones are still in place. This coefficient depends on the thickness and the material of the board.

- *Phase 2: Protection Phase*

The length of this second phase depends on the ability of the protection to stay in place during the fire and the time that marks the end of this phase is the t_f (fall-off time) as shown in the *Graph 1*. In this case it's possible to assume that the protection board has the same protection as cases of rectangular cross-sections TFA, so the information already found is used. For timber I-joists and its protection boards it's assumed that the protection they offer is the same as in TFA with rectangular cross-sections and the coefficients of fall-off time and k_2 are obtained from relevant literature or the testing of TFA.

Note: TFA means Timber Frame Assemblies.

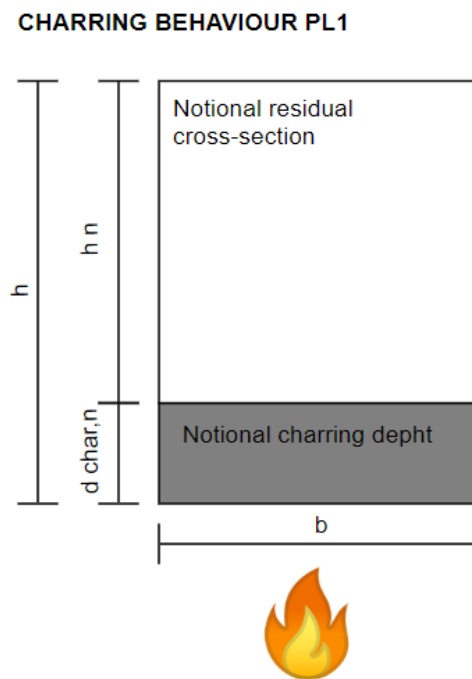
- *Phase 3: Post-protection Phase*

In this case the charring rate is influenced by the type of insulation applied in the timber and filled in its cavities. Before this study Tiso (Tiso, 2018) described an updated charring model for rectangular timber elements in TFA insulated with different cavity insulations. The protection level of the insulation is evaluated with a model-scale furnace fire test. The test consists in model-scale furnace fire test where the length of it should be about 60 minutes and the fall-off of the protective board should be induced at 45 minutes. When the test finishes the necessary coefficients are obtained according to the measure of the charring timber member. [10]

4.5.1 Protection Levels (Tiso 2018)

Once the results of the tests are obtained its insulation has to be qualified into a protection level which is based on model-scale furnace fire test following a standard time-temperature curve. We can qualify the three different levels (Tiso 2018).

PL1 : The insulation material protects the lateral sides of the timber member and the charring only happens in the frontal part. The *Picture 6* shows how this charring happens in PL1.

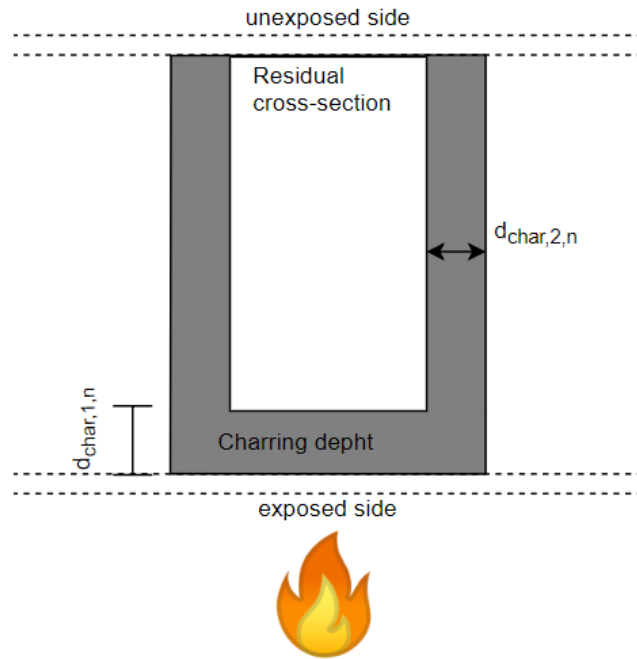


Picture 6: Charring behavior PL1

PL2 : The lateral charring reaches de 2/3 parts of the total side height of the timber member during the post-protection phase. The *Picture 7* show how this charring happens in PL2.

PL3 : The charring occurs during the protection phase so the insulation doesn't give any protection to the timber member. These types of insulations melt at temperatures lower than 300°C. The *Picture 7* show how this charring happens in PL3.

CHARRING BEHAVIOUR PL2/PL3



Picture 7: Charring behavior

For understanding the model developed by Tiso in 2018 is need to know about the formula of the charring depth along the fire-exposed side $d_{char,1,n}$ and its parameters of the current method given in the EN 1995-1-2 and defined by the *Formula 5*.

$$d_{char,1,n} = \beta_0 \cdot k_{s,n} \cdot k_2 \cdot (t_f - t_{ch}) + \beta_0 \cdot k_{s,n} \cdot k_{3,1} \cdot (t - t_f)$$

Formula 5 : charring depth along the fire-exposed side

Where:

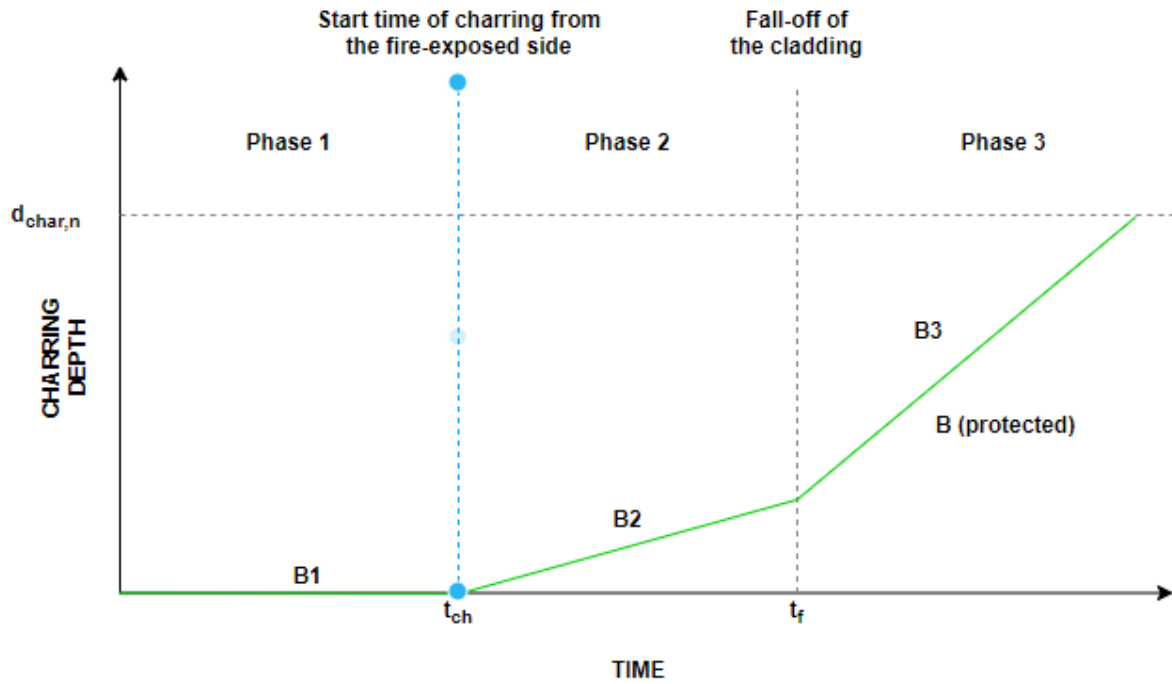
- β_0 : is the basic (or one-dimensional) design charring rate.
- $k_{s,n}$: is the cross-section factor being used to consider the influence of cross-section dimensions on the charring rate.
- t_{ch} : is the start time of charring on the fire exposed side behind the protection board.
- $t_{ch,2}$: is the start time of charring on the lateral sides.
- t_f : is the fall-off time of the protection board.
- k_2 : is the factor taking into account the protection offered by the protection board while it is in place.

- $k_{3,1}$: is the factor for charring depth along the fire-exposed side taking into account the protection offered by the protection board and insulation in post-protection phase.
- $k_{3,2}$: is the protection factor for the charring on the lateral sides in the post-protection phase.
- t : is the fire exposure time.

In our study the principal objective is to find the parameter $k_{3,1}$, which defines the charring depth along the fire-exposed side taking into account the protection offered by the board in post-protection phase.

This parameter only affects the PL1, the protection level which defines the case where there is a burning time that the timber member doesn't suffer directly the charring because the protection board. During an initial time interval that can vary from a few minutes to 1 hour or even more, the protection board material suffers the full load that the fire causes. During this interval the protection board material is charred and depending in its thickness, the time before the fall of the protection board and the temperature it gets the timber member can be charred or not. The parameter $k_{3,1}$ defines this situation.

The parameter $k_{3,1}$ measures the capacity and power with which the fire burns and carbonizes the timber once the protection board has been burned. In this case, the cavities are completely filled with stone wool insulation and then carbonization is produced mainly on the fire-exposed side of the timber member while the sides are protected by that stone wool insulation. The *Graph 2* shows the charring steps in PL1.



Graph 2: Charring of timber members in TFA with PL1 cavity insulation

The importance of the $k_{3,1}$ factor is that it takes into account the influence of the increased charring rate on the fire-exposed side of the timber member after the protection board has fallen off. The type and form of the cavity insulation affect directly this factor. The $k_{3,1}$ is expressed as a function of the fall-off time t_f of the protection board. The values were developed based on unloaded model-scale furnace fire tests and thermal simulations which are shown later.

In the thermal simulations it is necessary to confirm that the Post-protection factor for charring along the fire-exposed side $k_{3,1}$ takes into account the protection offered by the cavity insulation in the post-protection phase. The current factors may be valid for the fire-exposed flange of a beam, in our case an I-joist. [10]

5 I-JOIST

5.1 General

I joist made of timber is the type of beam it's been analysed in this study. The I-joist is a modern product designed to replace the traditional timber joists with an effective and safety way. I-joist gives a solution with lots of advantages and reduces the most common problems at the same time of the traditional structures. It was invented in 1969, during the reactivation of the world of timber structures and since then is the most used joist in the timber structures world. Its beginning was timid but little by little it has completely replaced the design of traditional timber structures and has been defined as the system to be used in all timber structures built today.

One of its most important advantages is that with a relatively small and optimized size and weight, this I-joist can have a very high strength. The biggest notable difference from dimensional lumber is that the I-joist carries heavy loads with less lumber than a dimensional solid timber joist. This advantage permits to build more strength structures with less material. As of 2005, approximately 50% of all timber light framed floors used I-joists. I-joists were designed to help eliminate typical problems that come with using solid lumber as joists. In the *Picture 8* and *9* shows a Solid lumber and an I-joist. [11]



*Picture 8 : Traditional timber beam,
photo from
www.robisonconstruction.co.uk*



*Picture 9 : I-Joist, photo from
www.twperry.com*

The advantages and properties of the I-joists are that they are less likely to bow, crown, twist, cup, check or split as would a dimensional piece of lumber respectively with the common joists. The I-joist dimensional soundness and little or no shrinkage help eliminate squeaky floors, avoiding these sound problems of the other conventional floors of timber. [12]

The I-joist consists only with two parts, the web and the flange, so its structure is very simple. The web is the large part in the middle, sandwiched between a top and a bottom flange and in a vertical position it creates the I shape. The flange has many options to be made because is the part which has less complex stresses. It can be made with laminated veneer lumber or solid timber finger-joined together for ultimate strength. This last part has a groove in the middle that fits and receives the web. The web has as well much kind of materials to be made, like plywood, laminated veneer lumber, or oriented strand board. With the correct sizing the assembled is made with water-resistant glue pressing the web into the top and bottom flange. [13]

Sizes vary according to the I-joist's intended load and span. Depths can range from 235 to 610 mm and reach up to 24 m in length, although 12 to 13 m is more common. The intended use for an I-joist is for floor and roof joists, wall studs and roof rafters in both residential and commercial construction. [13]

The material and its shape are simply, but its installation is not. So in all the constructions it is needed to have to take care about all the procedures, the misplacing and the improperly sizing to avoid mistakes. The lightweight nature of I-joists makes them more vulnerable to fire than dimensional lumber because its size is usually thin. A study made by Underwriters Laboratories found that structural assemblies composed of I-joists usually fail significantly with less time under fire effects than those which are made by dimensional lumber. Fire provokes failures of lightweight trusses and I-joists have led to the deaths of several fire-fighters. The *Picture 10* shows the effect of the fire in an I-joist and understands the effect it takes in the whole structure and its resistance. [14][15]



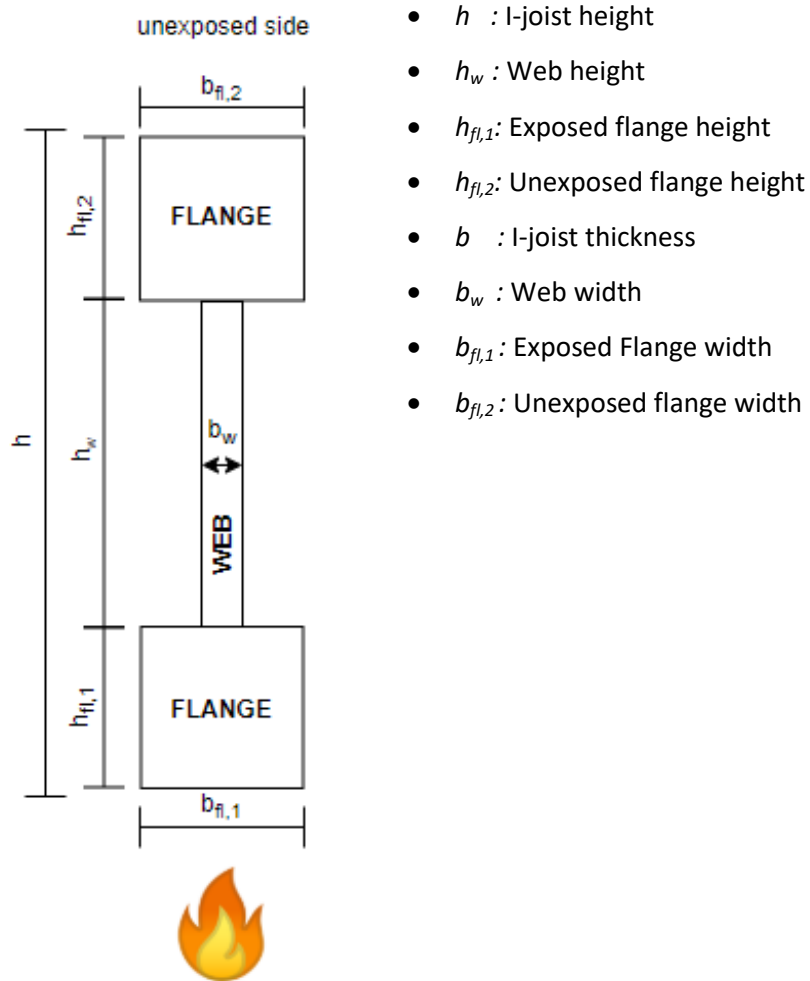
Picture 10 : I-Joist burned by fire, photo from www.pinkwood.ca/why-fire-rated-a

To avoid these dangerous situations it is obligated to do an exhaustive study and simulations to find solutions for the I-joists in case of fire. All these actions ensure progress in the development of creation and protection of new I-joists.

5.2 I-joist Parameters definition

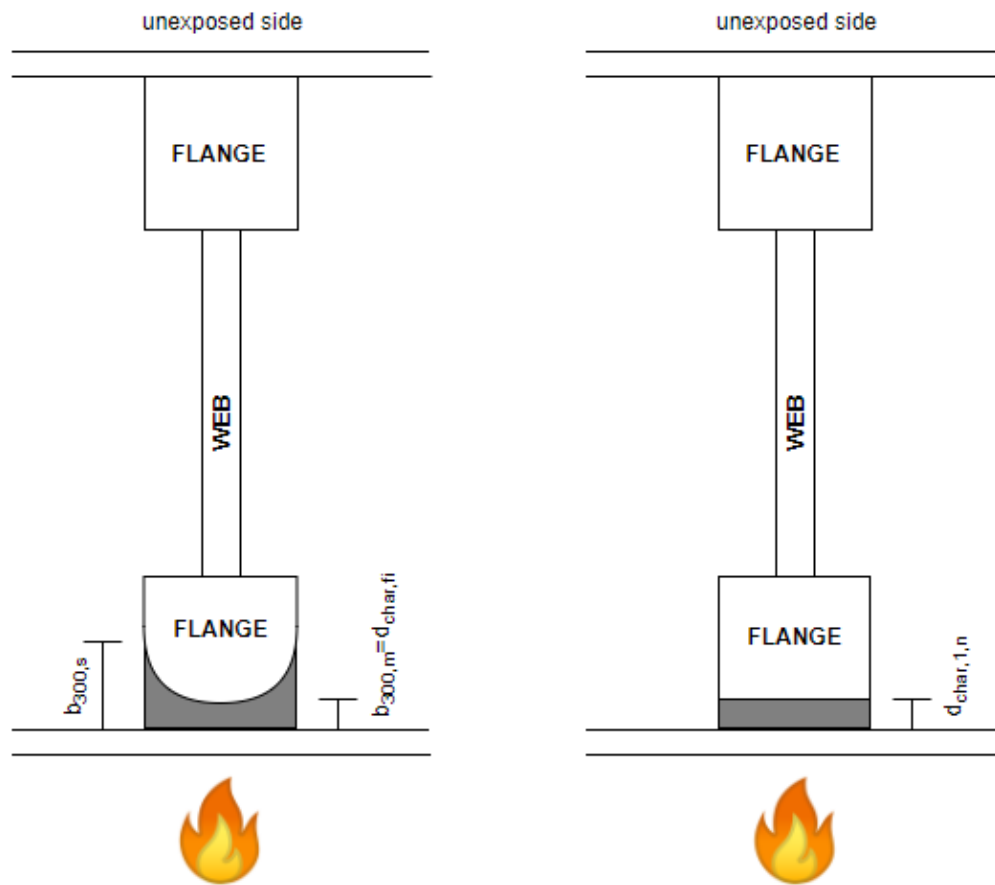
Once I-joist is defined, is necessary to know the parameters that define it both in form and components and when it is under the effects of fire and begins to evolve as time passes. The studied case only defines the components that affect the phenomenon of carbonization, since in the reduction of properties is not taken into account in this study.

The parameters and the physical measures of a timber I-joist are shown in *Picture 11*.



Picture 11: I-Joist Components

And on the other hand the naming of the parameters of the charring in an I-joist shown in *Picture 12*.

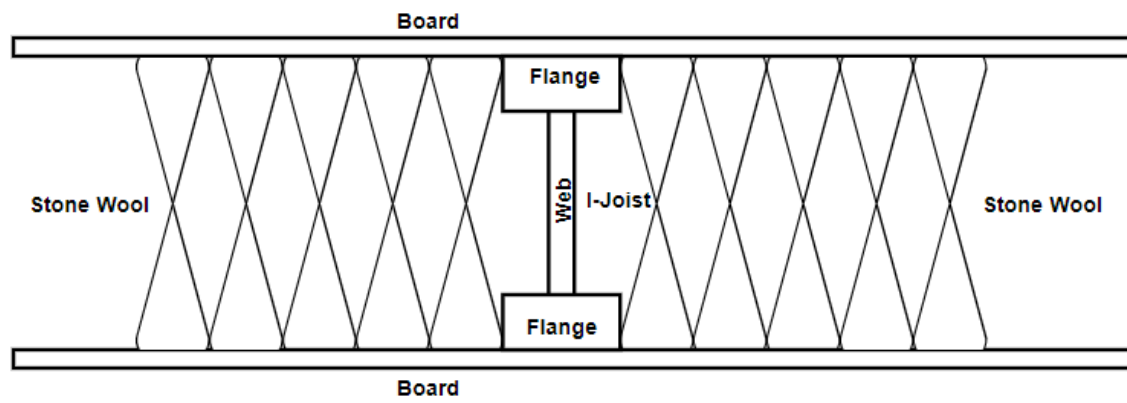


Picture 12: I-Joist under the fire parameters

- $b_{300,s}$: Maximum charring in the side of the cross-section
- $b_{300,m} = d_{char,fi}$: Minimum charring part in the middle of the cross-section
- $d_{char,1,n}$: Charring reduction to the minimum value at the middle part

[10]

And apart from the timber structural members, an insulation material is filled in the empty cavities between all the I-joists to make more resistant against fire the timber structure. In our case the insulation material is the stone wool. In the *Picture 13* shows how the stone wool is filled between the I-joists and the protection boards.



Picture 13 : Front view of timber structure components.

6 DETERMINATION OF $K_{3,1}$ EQUATION

6.1 Thermal Simulation

The first part of the study and the first information and data obtained come from the Safir thermal simulation program.

Note: First of all I must say that in this work does not include the simulations with Safir but if the results obtained from the simulations are used. In addition of being the first information used. Therefore it is necessary to comment on how the program works and how it affects the main topic of the work.

Safir is a program simulation developed to permit the modelling of the behaviour of the timber structures under the effects of the fire, it have lots of applications for a very large number of different cases. The main objective of this program is to analyse the timber structures in fire and determine its mechanic behaviour of this structure till the moment it fails. The structure could be made by a 2D skeleton of lineal elements like beams and columns, in our case I-joists, joined with plane elements like walls, slabs, roofs, etc. The volumetric elements could be used for the detail analysis of the structures, like the connections. It's possible to define the type of materials of the structures like steel, concrete, aluminium, but in our case timber is used for the structure and protection board and stone wool for the insulation materials.

In our case the I-joist is defined in the software platform with all his area and with the elements which join it in the structure, which are the other structural elements and the insulation material. All the components are defined for making the case as real as possible. The Safir software platform works with finite elements method so once the structure is defined all the structure is simulated with finite elements. That means that the program divides all the physical elements in thousands of nodes which have the same properties of the material.

Once the structure is prepared the fire is simulated affecting the structure like in real cases. Before the simulation we have to enter the data of the fires and the gas temperatures produced by the fire in the program following the International Normative (in the most cases we enter in the program curves of time-temperature). Then with those data and gas temperatures Safir calculates the evolution of the temperatures in the structure depending on the materials it is done, in our case the timber and the insulation material. Then these temperatures are stored in some concrete files.

Then the program calculates the mechanic behaviour of the structure from its geometry, hold conditions, the charges it is holding and the mechanic properties of the material (mainly the strength) taking into account that the fire rises the temperature as the time passes. The elevation of the temperature on the materials produces thermic elongations and charring next to a reduction of the strength and the rigidity of the I-joists. As a consequence, the displacements and in our case the charring of the structure rises during the fire till the collapse. The program at the end stores all the data of every node where the structure was divided, so it can know every state of every node in every moment of the analyses.

All the files obtained from Safir are organized depending on the thickness of the insulation material h_p and depending on the time of falling t_f of the protection board between the fire and the I-joist. In total 8 cases are analysed with different h_p and t_f . For each case of h_p and t_f all the existing sizes of I-joists are analysed depending on the width size of the exposed flange b , the height size of the exposed flange h and the length of all the I-joist H . In total ten types of flange profiles are analysed. Individually file shows mainly the node and its temperature in big tables. Maybe the structure is divided in 15000 nodes approximately, so 15000d data are obtained. And also in each file more than one interval of time is analysed in each case for h_p and t_f , so at the end a heap of endless data is obtained. The following expression shows how the data is organized.

Cladding thickness (h_p) > Failure Time (t_f) > Hbh > Time exposition > structural node

This is very useful but maybe at the end of the simulation more than a million of data is obtained and it is impossible to analyse all of it. For this reason all the data must be compiled and translated in a file analysable with the most commonly used variables for do the calculations of fires in timber structures in an easier way. An algorithm in Matlab is used for translating all this data. All of it is explained in the following chapter. [16]

6.2 Matlab Algorithm

Once the results from the Safir are obtained, all of them have to be translated to a simple and understandable file. The Matlab algorithm is used to obtain it. This Matlab algorithm gives an Excel file of results for any file of Safir we have. Each file obtained from Safir is defined by h_p and t_f , that means:

h_p : *thickness of protection board*

t_f : *time of falling*

And in each file there are ten type of I-joist shape Hbh, that means:

H : *length of the I – joist*

b : *width of the I – joist flange*

h : *height of the I – joist flange*

The Safir file have to be inserted to the Matlab algorithm and this one, after a few minutes gives the simplified file in Excel. Once the data processing is achieved it is easier to understand and use these initial data.

6.2.1 Matlab Flowchart

To better understand the procedure of Matlab algorithm as much as possible, it is represented with a flow chart with a brief explanation of each step.

This flowchart doesn't follow the traditional laws of the flowcharts as regards forms of the boxes it refers. It only shows schematically which the principal algorithm steps are and it gives briefs explanations about the modifications and actions made between the principal steps.

6.2.2 Flow chart explanation

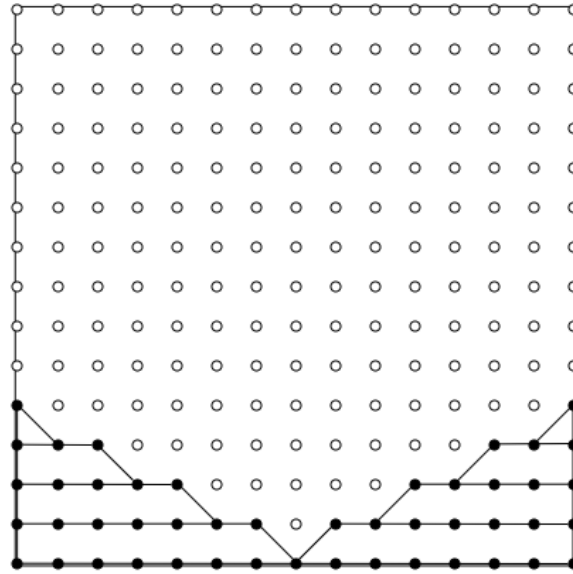
Firstly in the Step 1 the data needed in Matlab for the Excel file, the name of file and the thickness of the web of the I-joist (b_w) are entered. In the Step 2 the rest of the shape sizes, principally the sizes of the flange, which are the base and the height of both of the exposed and unexposed flanges (b_{fl} , b_{fl1} , h_{fl} and h_{fl1}), are entered.

Then the algorithm reads the Safir file which gives the simulation of the fire in the timber structure and combined with the first data entered the algorithm gets the data needed. In the Step 4 the algorithm reads the nodes information and differentiated the nodes between the exposed and unexposed flanges, the web nodes and all the repetitions. Once the nodes data is obtained, the algorithm in the Step 5 removes the useless information obtained in all the cases for each type of I-joist and structure. In the Step 6 the algorithm take care about the time for each case in the type of size of the I-joist and choose the useful information and fix it.

Once the useful information is fixed, in the step 7 the algorithm organizes this information in a table where the temperatures for each node are shown. The table changes its shape from Node-Temperature to the same but in vertically (in this way is easy to treat the information). And finally in the Step 8 the table is created.

Then in the Step 9 all the parts of the structures which are not the I-joist are removed and only the parts of the I-joist that can give useful information stay in place. Then the first check is made. In the Step 10 the three parts of the I-joist are separated to study them in parts, which is easier because at the end the more useful information comes from the unexposed flange. Maybe in the other parts the charring gives more information but the most affected part is the exposed flange.

The following steps finds the start time of the charring in the three parts during the fire. In the step 11 the start charring part of the web is found, then in the step 12 the start of charring time of the unexposed flange and then in the step 13 the start charring time of the exposed flange. The algorithm finds the start time of charring analysing all the nodes and looking for the node temperatures which rises the 300°C, which is the temperature when the timber starts charring. Then compiling all the data for each node the algorithm calculates the area of the charring for each time of the fire. The area is calculated by trapezoids, which means that the area made by the charring nodes is done by assume of trapezoids and the sum of its areas, like it is shown in *Picture 14*.



Picture 14 : Trapezoids Calculation Methods

The picture shows more or less the idea of how the charring area is calculated in each time of the fire in the Step 14. And then in the Step 15 the charring of the lateral sides is found, with the trapezoids calculation method as well.

Finally in the Step 16 and 17 the algorithm prepares and gives the results in an Excel file named before in the Step 1.

6.2.3 Results obtained by Matlab

Once the Safir file is run in Matab and the excel file is obtained, the data got for each size of I-joist, for an specific thickness of protection board and time of falling are join in a table where information is shown. The information got by the Matlab shows how the charring evolves during the fire since the protection board falls till the flange is completely charred.

The *Picture 15* shows the format of the files obtained and the information it gives.

	A	B	C	D	E	F	G	H	I	J	K	L	M	N	O	P
1	tch,w=			time	hres	A	hb									
2	tch,u=															
3																
4	tf=															
5	bfl=															
6	hfl=															
7																
8																
9																
10																
11																
12																
13																
14																
15																
16																
17																
18																
19																
20																
21																
22																
23																
24																
25																
26																

Picture 15 : Safir data from Matlab

In the green box contains the size information of the width and height of the flange of the I-joist, b_{fl} and h_{fl} , in millimetres, the time of start of charring and the protection board time of falling t_f , and the start charring of the web and the unexposed flange $t_{ch,w}$ and $t_{ch,u}$, all in minutes. Here the useful information is the three ones on the bottom part.

In the blue box there is the information needed to analyse and get results to find the $k_{3,1}$, so is the most important part. It shows the time in minutes where the charring is happening in little intervals of time. Then the h_{res} shows the height of the exposed flange where the charring does not started in each time of the simulation. The A shows the area which is not charring yet, calculated by the trapezoid method explained before. And the h_b shows the proportional height of the simplified charred area.

Finally in the red box there are all the different shapes and sizes of the I-joist flanges separated in different excel tabs.

6.3 Excel Analysis

Once the Excel file is obtained with all the data of the simulations, more data have to be obtained using the formulas known till now. The results to treat and which are important for the searching of the $k_{3,1}$ are principally the d_{char} and the time when it happens. With this information is possible to know which is the coefficient $k_{3,1}$ in one time. For find it the *Formula 6* is needed.

$$k_{3,1} = \frac{d_{char,1}}{\beta_0 \cdot k_s \cdot (t - t_f)}$$

Formula 6 : $k_{3,1}$ formula

Where:

$d_{char,1}$: height charred of the exposed flange of the I – joist

β_0 : charring rate

k_s : Cross section factor

t : time

t_f : time of falling of the cladding

Where:

$$d_{char,1} = h_{fl,1} - h_b$$

Formula 7 : Charring depth depending on the h_{res}

$h_{fl,1}$: total height of the exposed flange

h_b : height without charring in a concrete time

Formula 8 is for Cross-section factor k_s .

$$k_s = 6,65 \cdot b_{fl,1}^{-0,37}$$

Formula 8 : Cross-section factor

Note: The formula for the Cross-section factor is not the one which is shown in the Technical guideline for Europe for the Fire safety in timber buildings. The one which is shown below:

$$k_s = \begin{cases} 0,000167 \cdot b^2 - 0,029 \cdot b + 2,27 \\ 1 \end{cases} \quad \begin{cases} 38 \leq b \leq 90 \text{ mm} \\ b > 90 \text{ mm} \end{cases}$$

Still having the official formula we decided to change it because this factor makes lots of differences between the shapes of the I-joists which have a height bigger than 90 mm. This makes some dubious results and at the end we decided to use the same Formula 8 for all the profiles of I-joist.

And the coefficient β_0 is:

$$\beta_0 = 0,65$$

Once the Formula 6 is introduced into the excel all the $k_{3,1}$ for each time, for each I-joist profile, for each time of falling and for each thickness of protection board are obtained. This information is joined next to the data obtained from the Matlab algorithm, with the objective of having the information joined and organized. The file after the results have this distribution is shown in the Picture 16.

	A	B	C	D	E	F	G	H	I	J	K	L	M	N	O	P
1	tch,w=			time	hres	A	hb	d _{char,1}	Ks	K _{3,1}						
2	tch,u=															
3																
4	tf=															
5	bfl=															
6	hfl=															
7																
8																
9																
10																
11																
12																
13																
14																
15																
16																
17																
18																
19																
20																
21																
22																
23																
24																
25																

Picture 16 : Results with Matlab data

In the yellow box contains all the results of $k_{3,1}$, the k_s and the $d_{char,1}$ for each time. But before getting the graphs, there is a problem in the results of the coefficient $k_{3,1}$, principally in the first results when the interval of time is 0 or extremely little.

6.3.1 Problem solution for first values

The results of the coefficient $k_{3,1}$ in the first cases sometimes are 0 or infinite, event that don't have any logic. To know better why this dubious results are obtained the equation have to be analysed more deeply, so for any variable this results are obtained:

- β_0

β_0 don't provoke problems because its value is constant and positive.

- k_s

For k_s an interval of values is obtained depending on the base of the exposed flange. With the minimum and the maximum values of the width of the size flanges is possible to check it.

$$b_{fl,1 \min} = 38 \text{ mm}$$

$$b_{fl,1 \max} = 140 \text{ mm}$$

For these two values the maximum and the minimum k_s can be obtained respectively:

$$k_{s \max} (b_{fl,1 \min} = 38 \text{ mm}) = 1,731$$

$$k_{s \min} (b_{fl,1 \max} = 140 \text{ mm}) = 1,0685$$

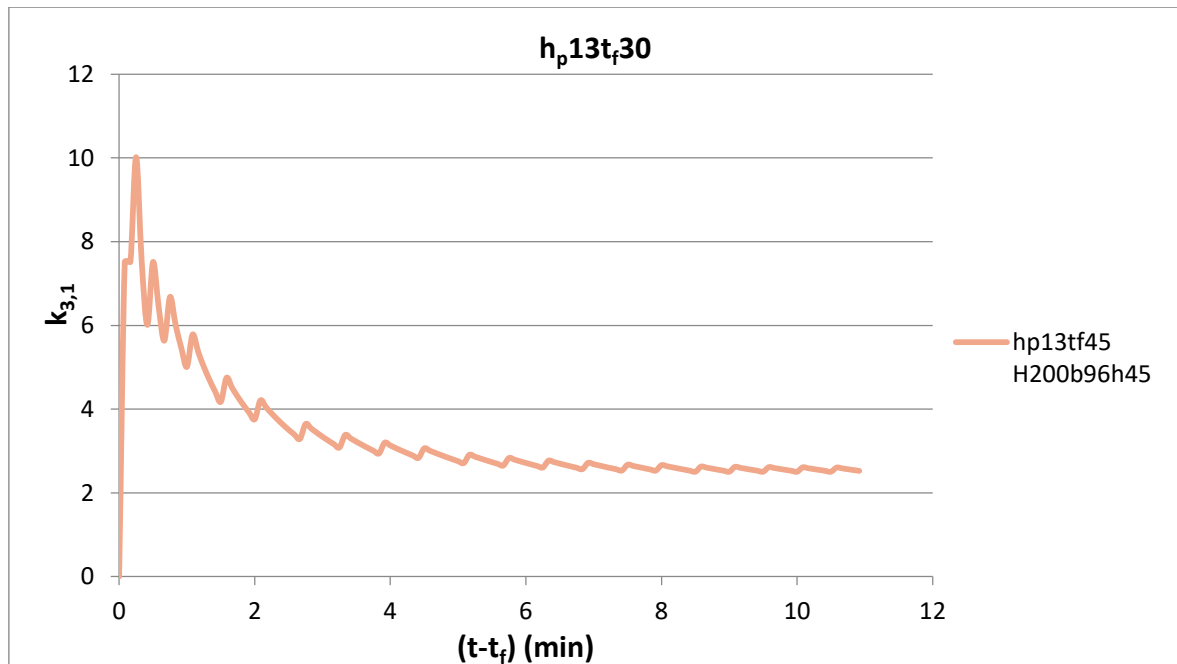
So this case shows that the minimum and maximum values are within a range of low and positive values that are not going to define $k_{3,1}$ as a 0 or infinite.

- $(t-t_i)$

For the range of time $(t-t_i)$ the first value is going to be 0 because $t=t_i$. This means that all the first values of $k_{3,1}$ in all of the cases tend to infinity. This is the first case that causes errors in the first values. I decided to get the results not starting in 0, but I decided to start in the second value where the time is not 0, that would give a logic number in the coefficient $k_{3,1}$. This problem appears in all cases so the $k_{3,1}$ must be calculated starting always with the second value.

- $d_{char,1}$

For $d_{char,1}$ there are values since 0 to all the $b_{fl,1}$, so it's possible to have a 0 in the nominator of the formula, and that can gives a 0 as a result for the coefficient $k_{3,1}$. Being the only value in this part converts the $d_{char,1}$ in the responsible of having a 0. This value, knowing that in the first value must be a infinite is totally illogical and must be corrected. If not a graph like the *Graph 3 is obtained*.



Graph 3 : Example $k_{3,1}$ Graph

There are three cases that act like in the *Graph 3* for $d_{char,1}$ values :

- h_p15t_f30 in all I-joist flange shapes (in t_0 and t_1)
- h_p15t_f30 in all I-joist flange shapes (in t_0 and t_1)
- h_p15t_f30 in all I-joist flange shapes (in t_0 and t_1)

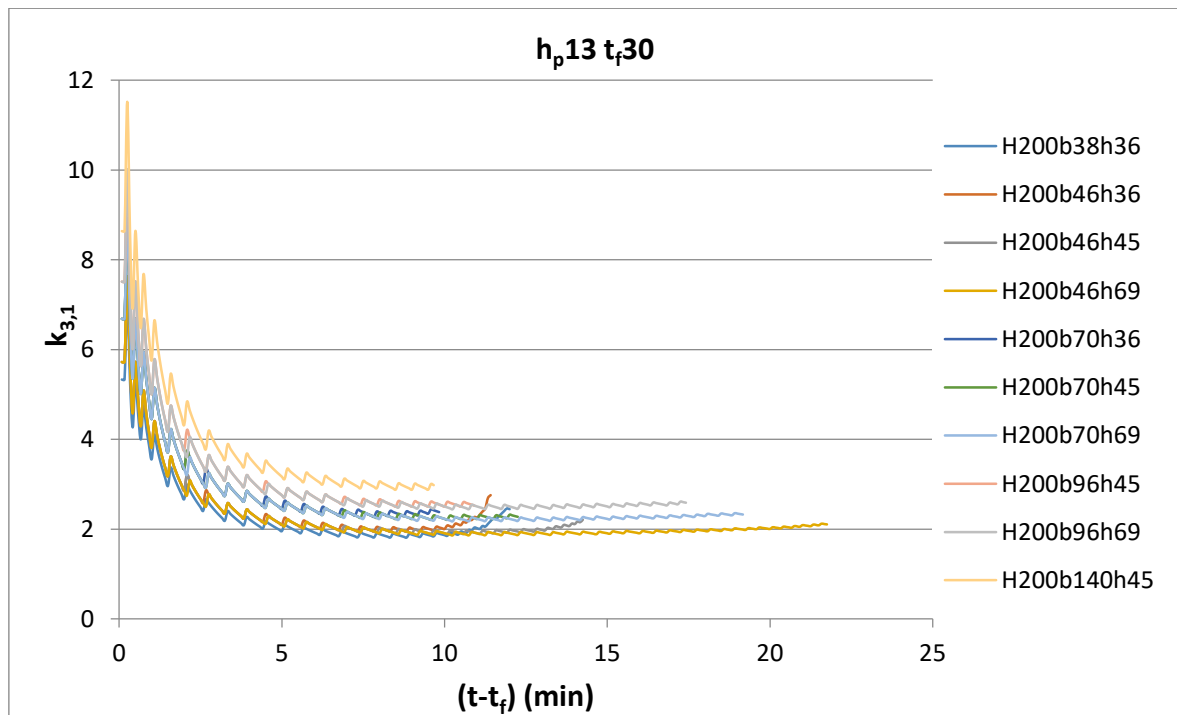
So it must be corrected, because all the graphs with the same tendence are needed. The solution is to put a low value of $d_{char,1}$ in each case for simulating a low charring depth in the flange. It is not correct at all because we are inventing those data, but is correct in part because the charring don't evolves millimetre per millimetre, its evolution is continuous and it could have decimals in its values.

Once corrected the problems in all data files the correct graphs with a similar tendency can be obtained and the final formula of $k_{3,1}$ can be founded correctly.

6.3.2 Graph

The objective of getting all of this data is to find a formula that gives the $k_{3,1}$ for all cases. So the next step is to compress all the data in the form of graphs for each profile in each document to make it easier to understand the information. The graph shows the coefficient $k_{3,1}$ depending on the advance of the time since the protection board falls. The curve obtained for each profile of I-joist flange also depends on specific protection board thickness and time of fall.

One example of a graph could be the *Graph 4*.



Graph 4 : Example case h_p13t_f30 Graphs

All shapes have a similar tendency when the I-joist is in fire and it is charring. The shape of the curve follows this way because the effect of the fire is stronger when the insulation material has fallen and the timber has no protection at this moment, so the coefficient $k_{3,1}$ is bigger in the first interval of time. Then the timber starts its charring and the carbon layer created acts as a protection layer, so the coefficient $k_{3,1}$ decreases and stabilizes as the time goes by. This is only a general explanation of the $k_{3,1}$ tendency, all cases have different values, different maximums and

minimums and more or less pronounced slopes, always depending on the characteristics of the protection, time of fall and dimension of the I-joist.

The curve has the typical tendency of a potential curve, so for each group of data a potential curve must be defined as that obtained. Once all the equations of the curves with the trend of potential type are obtained, they are grouped and stored in Table 1.

$h_p 13t_{r30}$	
Size	Equation
H200b38h36	$y = 3,442x^{-0,273}$
H200b46h36	$y = 3,7159x^{-0,283}$
H200b46h45	$y = 3,6645x^{-0,275}$
H200b46h69	$y = 3,4569x^{-0,222}$
H200b70h36	$y = 4,4061x^{-0,311}$
H200b70h45	$y = 4,3541x^{-0,299}$
H200b70h69	$y = 4,1395x^{-0,245}$
H200b96h45	$y = 4,9302x^{-0,311}$
H200b96h69	$y = 4,7226x^{-0,26}$
H200b140h45	$y = 5,6965x^{-0,321}$

Table 1 : Equations for each size

And the *Formula 8* shows the basis equation for all cases:

$$k_{3,1} = M \cdot t^N$$

Formula 9 : Basis equation for $k_{3,1}$

Where:

$k_{3,1}$: is the factor for charring along the fire exposed in the postprotection phase

M : parameter that marks the starting value and the tendency of values

t : time

N : parameter that marks the trend of stabilization of the curve

The next step is combine this limited number of equations of each size I-joist shape (there are 10 I-joist sizes per case normally) and makes a unified equation with all the data compiled on it.

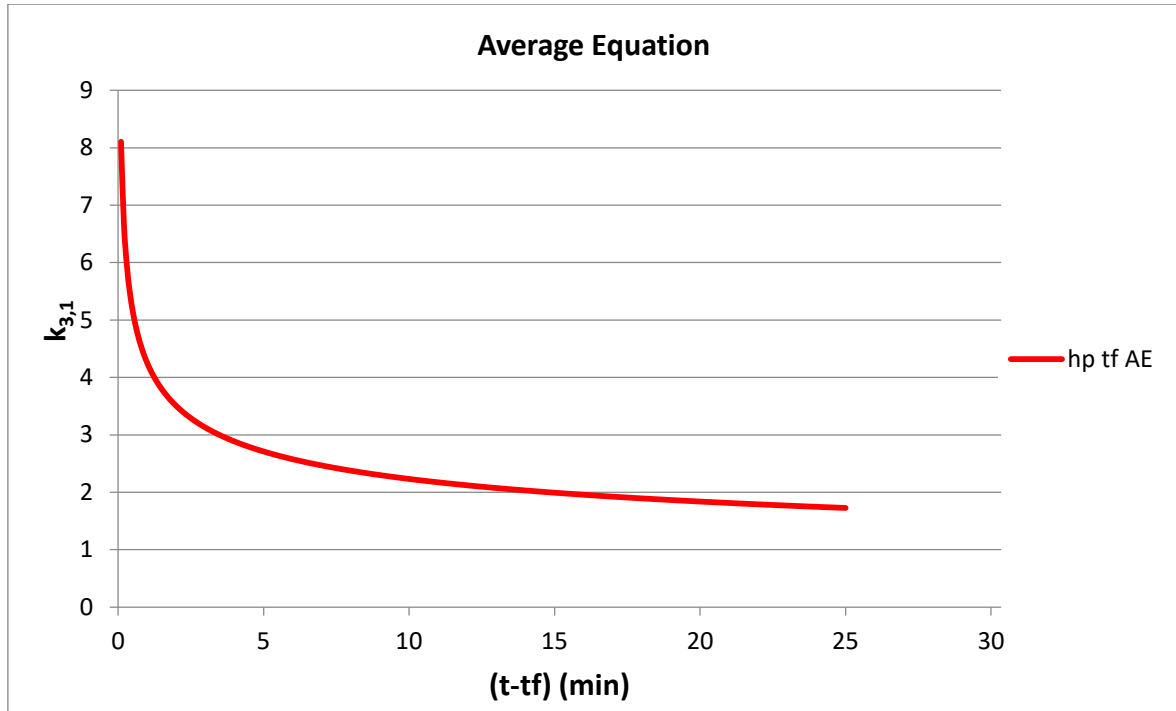
Having all the graphs with a tendency very similar to the rest for each specific h_p and t_f , the best option was to make the average of the parameters A and B of the equations obtained in each case and obtain the Average Equation.

The values obtained are shown in the *Table 2* with the averages necessities to know and the Average Equation obtained.

Average Equation $h_p, 13t_f, 30$	Parameters	
Size	M	N
H200b38h36	3,442	-0,273
H200b46h36	3,7159	-0,283
H200b46h45	3,6645	-0,275
H200b46h69	3,4569	-0,222
H200b70h36	4,4061	-0,311
H200b70h45	4,3541	-0,299
H200b70h69	4,1395	-0,245
H200b96h45	4,9302	-0,311
H200b96h69	4,7226	-0,26
H200b140h45	5,6965	-0,321
Average	4,25283	-0,28
Average Equation	$k_{3,1} = 4,2528 \cdot t^{-0,28}$	

Table 2: Average Equation for one case of $h_p t_f$

Once the Average Equation is obtained the values that it gives have to be represented to analyse them.



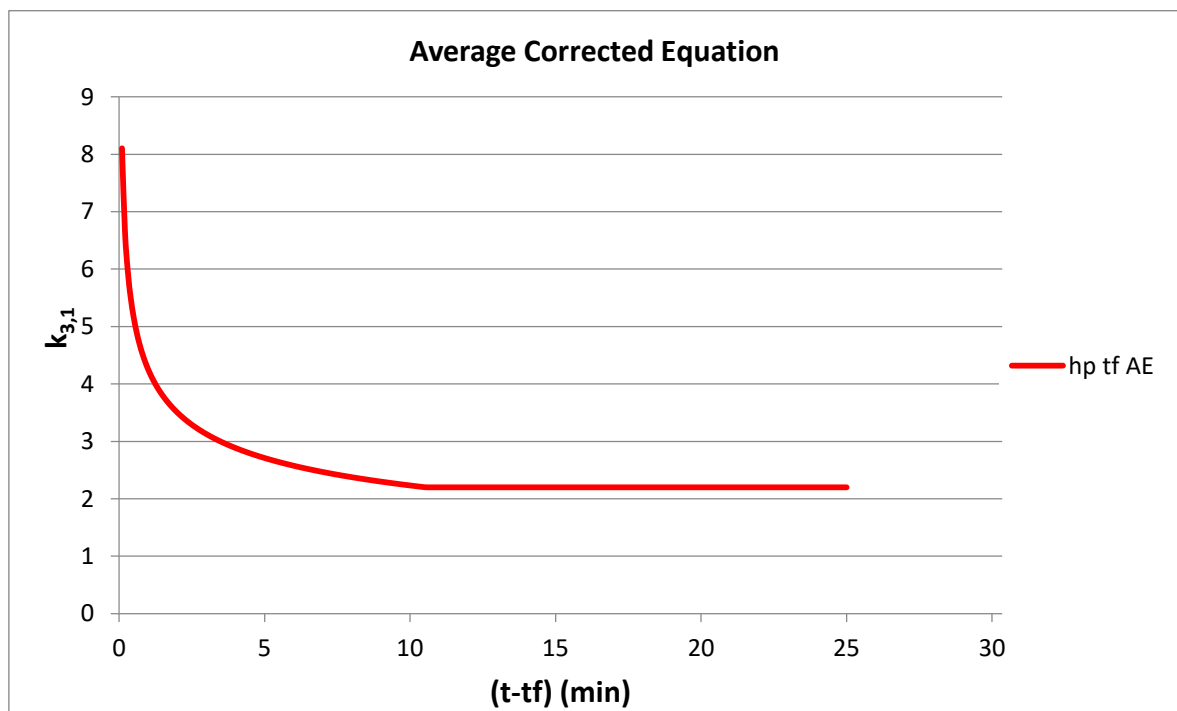
Graph 5 : Example Average Equation Graph

This is the graph of the Average Equation for all the I-joist shapes obtained in the simulations. The tendency and the values are really close to the values taken from the simulation, but there is a problem in getting the curve directly from all the equations. In the stabilization interval the values tend to a lower minimum compared to the minimum obtained in all the results of each dimension of the I-joist, therefore it is necessary to modify this trend. From the results obtained from the average curve a minimum is set where the data cannot be smaller, and from there iteration is done, taking another potential curve more reliable to the obtained results. That minimum is the average of the minimums of the simulations for each size of I-joist. The *Table 3* show it.

Size	$K_{3,1 \text{ min}}$
H200b38h36	1,8111
H200b46h36	1,9437
H200b46h45	1,8911
H200b46h69	1,8612
H200b70h36	2,2758
H200b70h45	2,2090
H200b70h69	2,1740
H200b96h45	2,5046
H200b96h69	2,4435
H200b140h45	2,8798
Average	2,1994

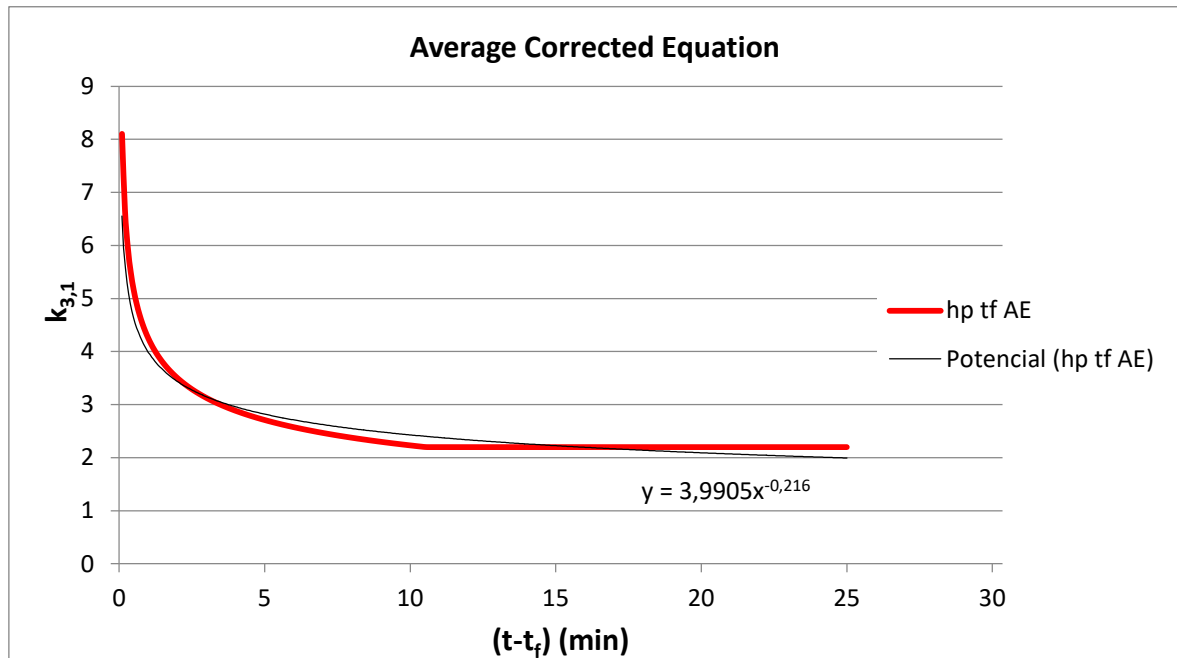
Table 3 : $k_{3,1 \text{ min}}$ average

Once the general $k_{3,1 \text{ min}}$ is obtained, it have to be introduced in the values obtained with the Average Equation. To stabilize the values the minimum value is fixed in the average minimum of all the $k_{3,1}$ found in each dimension of I-joist and thus stabilize the general graph of the $k_{3,1}$. The Graph 6 shows it.



Graph 6 : Example Corrected Average Equation

In the last graph the last values are stabilized in the minimum average. Then another trend line is obtained on the new graph that shows a new tendency of $k_{3,1}$ this time more stabilized in the final values, that is closer to the graphs obtained at the beginning for each dimension of I-joist. The *Graph 7* shows this modification.



Graph 7 : Correction of Average Correction and General Equation

With the tendency line its minimum is found and verifies that it is within the minimum range of all $k_{3,1}$ of each dimension of I-joist. If so, then is possible to say that the General Equation found is reliable. This prove is shown in *Table 4*.

General Equation	$y = 3,9905x^{-0,216}$
m	3,9905
n	-0,2160
Minimum value	2,0119
Maximum $k_{3,1min}$	2,8798
Minimum $k_{3,1min}$	1,8111

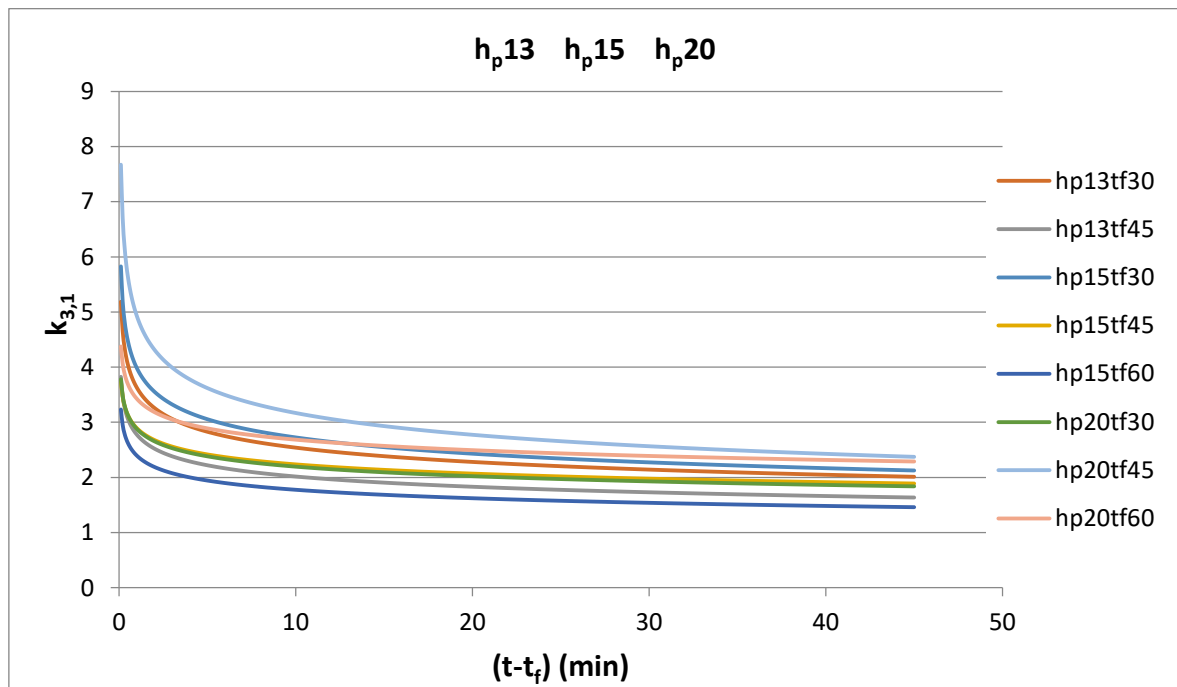
Table 4 : $k_{3,1min}$ comprobation

In this case the General Equation founded is valid for this case and the following work and analysis is done with this equation. All this procedure has to be done for each of the cases that depend on

h_p and t_f . In all the cases this result is valid. Once all the General Equations are obtained the next phase of analysis can be started.

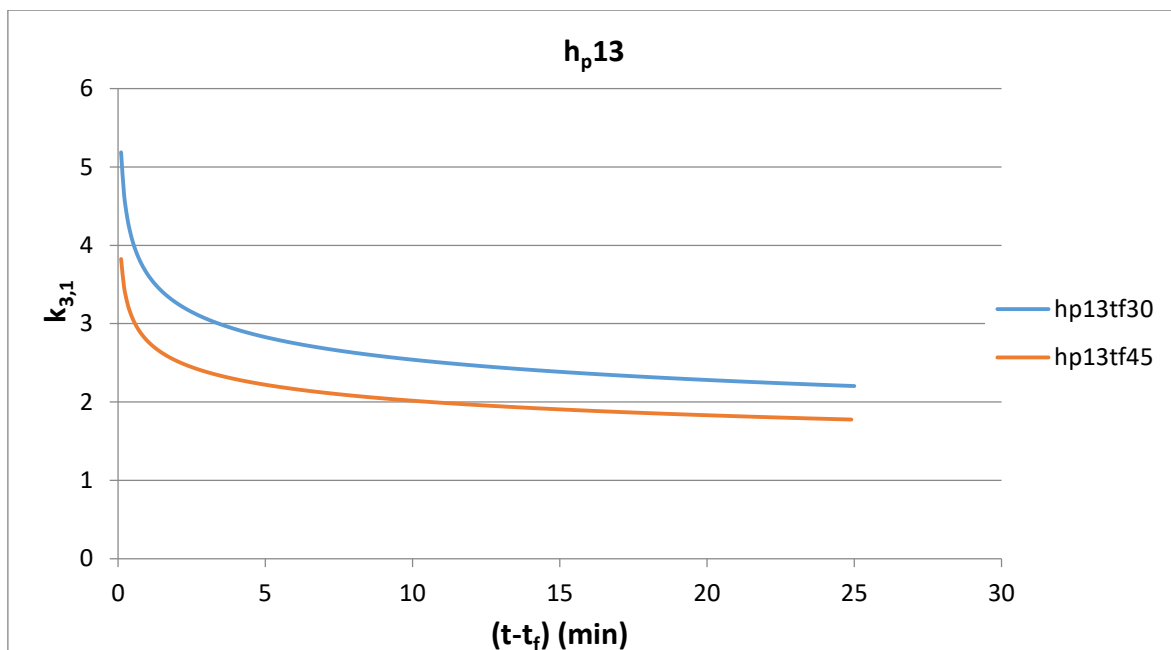
6.3.3 General Equations and Graphs

With all the General Equations for all the cases we express them in a graph for analyse its tendency, as we show in the *Graph 8*. Once we arrive at this point we work always with the General Equation.

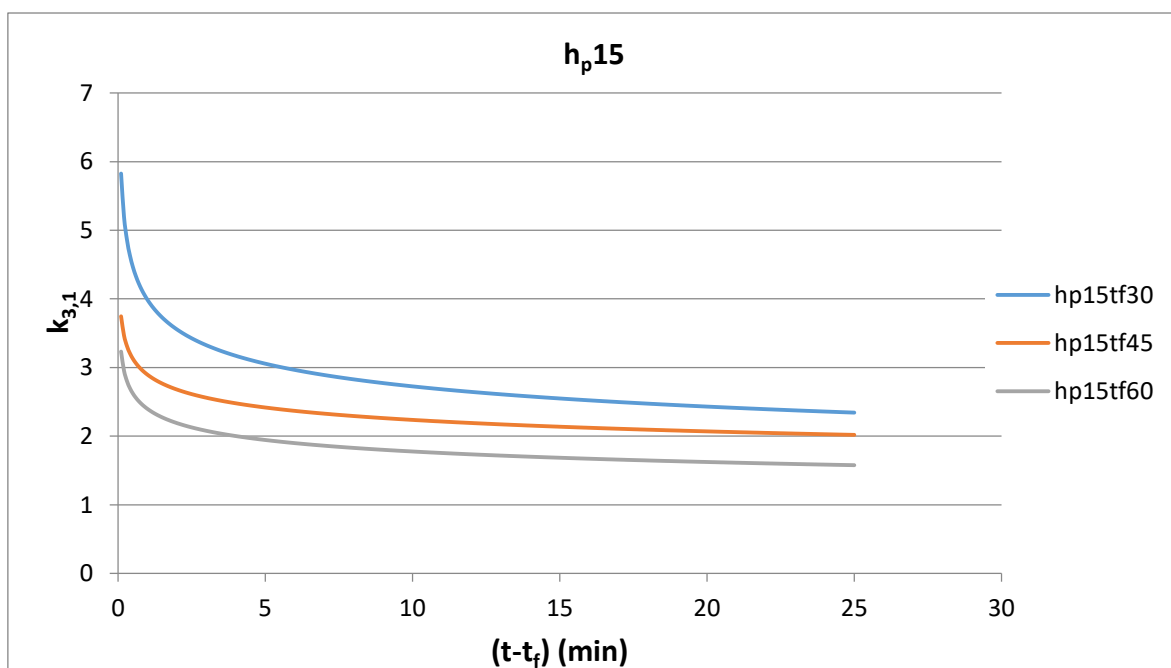


Graph 8 : All graphs from one case $h_p t_f$

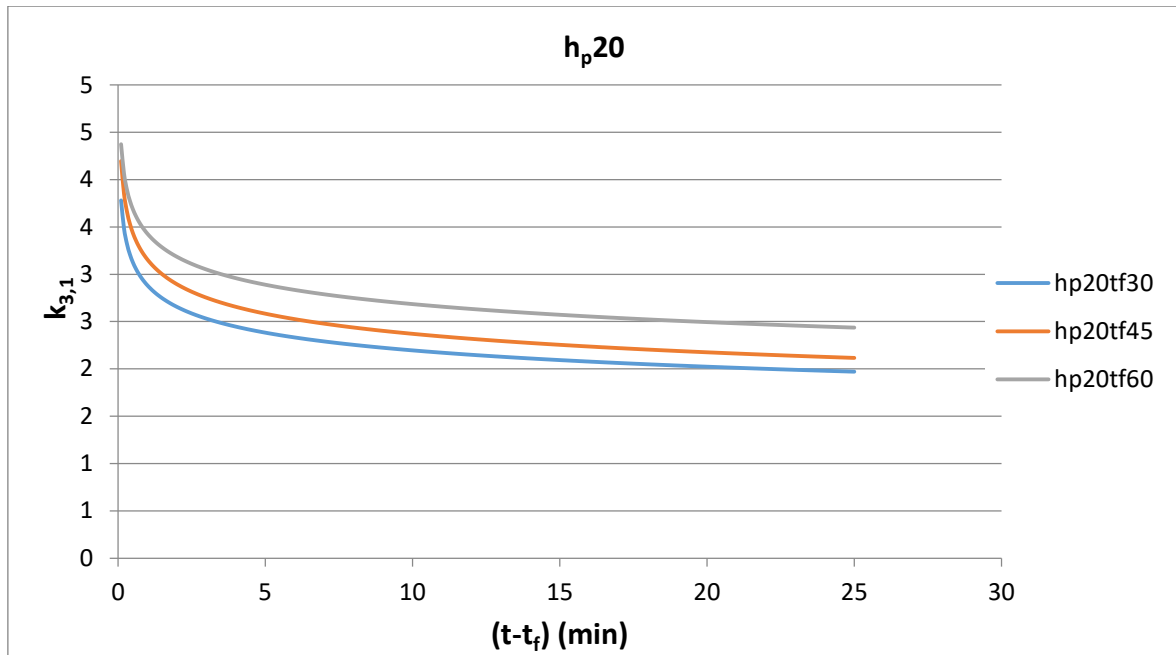
As it can be seen, indeed all the graphs follow a similar tendency and that is good sign since it shows that all simulated timber structures tend to react in the same way as the effects of fire. With their respective differences depending on h_p i t_f . To see each case with more perspective it can be seen that in the *Graphs 9, 10, 11* depending on each h_p and see if the results follow a logical order.



Graph 9 : General equations h_p13



Graph 10 : General Equation h_p15



Graph 11 : General Equation h_{p20}

As it can be seen in the first two graphs, the magnitude of the values depending on t_f is correct because as more time it takes for the protection board to fall, the smaller the coefficient $k_{3,1}$ is. That has its logic because as less time of fall less carbonization originates in the first layer of timber before the protection board protection falls or simply does not create carbonization. Therefore the timber does not have that protective layer of carbon and the effects of fire are more powerful and important at the beginning, and therefore the $k_{3,1}$ is greater. And for those graphs the General Equations in the Table 5.

General Equations		
$k_{3,1}=M*t^N$	M	N
h_{p13t_f30}	3,6296	-0,1550
h_{p13t_f45}	2,7773	-0,1390
h_{p15t_f30}	3,9850	-0,1650
h_{p15t_f45}	2,8947	-0,1120
h_{p15t_f60}	2,3963	-0,1300
h_{p20t_f30}	2,8814	-0,1180
h_{p20t_f45}	4,9300	-0,1920
h_{p20t_f60}	3,4272	-0,1060

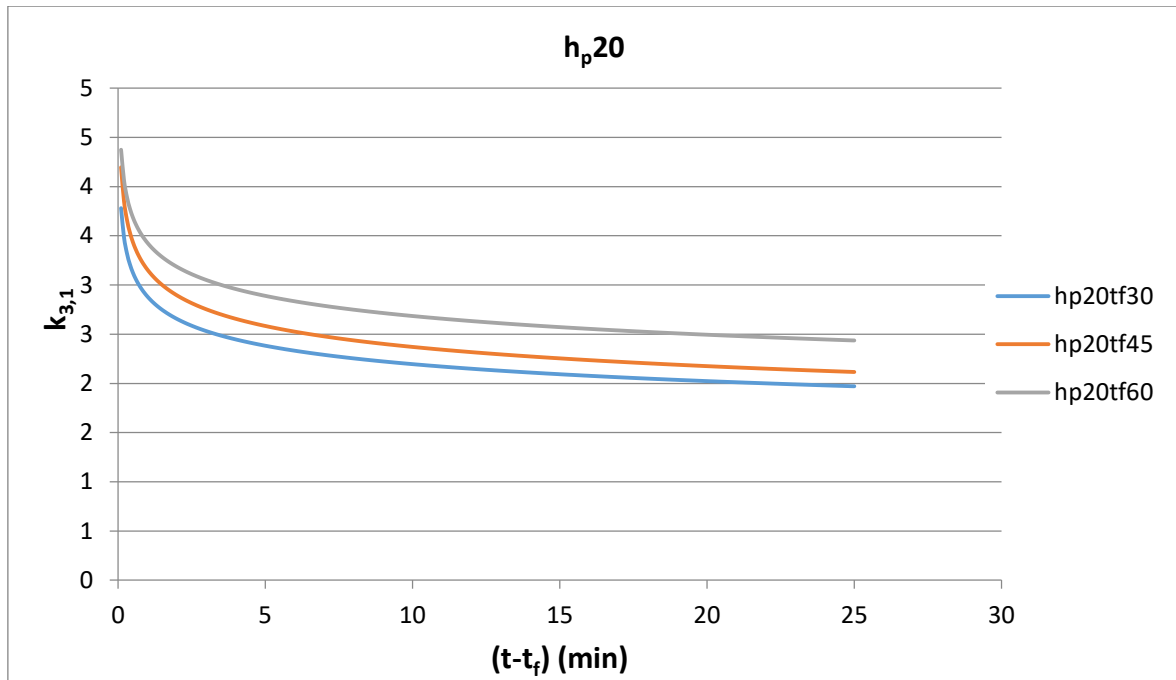
Table 5: General Equations

But then in the last case, where the h_p have a thickness of 20 mm the values of the parameter $k_{3,1}$ has no logic in comparison of the other ones. The graph shows that the case h_p20t_30 have lower values than the other ones. This happens because in the latter case the h_p is larger than in the other cases and the evolution of the timber under the effects of the fire is different. The main difference is that the timber never gets carbonized before the insulation falls, therefore the protective carbonization layer is not created, therefore the $k_{3,1}$ parameter tends to be higher. The *Table 6* shows better the tendencies.

Average			
Size	d_{char} (mm)	$K_{3,1}$	$K_{3,250}$
h_p13t_30	2	8,83	2,20
h_p13t_45	19	3,71	2,11
h_p15t_30	0	6,62	2,11
h_p15t_45	12	4,01	1,88
h_p15t_60	38	1,87	0,98
h_p20t_30	0	6,61	1,96
h_p20t_45	0	13,28	2,66
h_p20t_60	0	6,22	2,05

Table 6 : Averages of initial d_{char} and $k_{3,1}$ and final $k_{3,1}$

Anyway, in the latter case the correct tendency is not followed, especially in the case h_p20t_45 where the $k_{3,1}$ in the initial values are exaggeratedly large compared to the other two cases with the thickness of the protection 20 mm. Therefore, in this case, I decided to vary these values since those obtained in the simulation I consider are not correct. I have obtained the new values through an interpolation of the other two cases. This change has been necessary because the data did not follow a logical trend and it does not consider it good for the final results. After correcting the case equation h_p20t_45 the *Graph 12* is corrected as it can be seen below.



Graph 12: General Equation h_{p20} corrected

And then the new General Equations (Corrected) are the following ones in the *Table 7*.

General Equations (Corrected)		
$k_{3,1}=M \cdot t^N$	M	N
$h_{p13t,30}$	3,4990	-0,155
$h_{p13t,45}$	2,7773	-0,139
$h_{p15t,30}$	3,5900	-0,165
$h_{p15t,45}$	2,8947	-0,112
$h_{p15t,60}$	2,3963	-0,130
$h_{p20t,30}$	2,8814	-0,118
$h_{p20t,45}$	3,1543	-0,124
$h_{p20t,60}$	3,4272	-0,106

Table 7: General Equations

Now the parameters that define the case $h_{p15t,45}$ are closer to the other ones so now the values are better to analyse all cases.

6.4 $k_{3,1}$ Formula

Once all the data joined in a coherent way, the main objective of the study is to look for a formula that gives the values of $k_{3,1}$ depending directly on the variables time t , thickness of the protection board h_p and time of fall of the insulation t_f because now the coefficient $k_{3,1}$ can be only found through the information collected with the Safir program. This formula makes it easier to know the coefficient $k_{3,1}$ only with these values, something that currently is not possible to do.

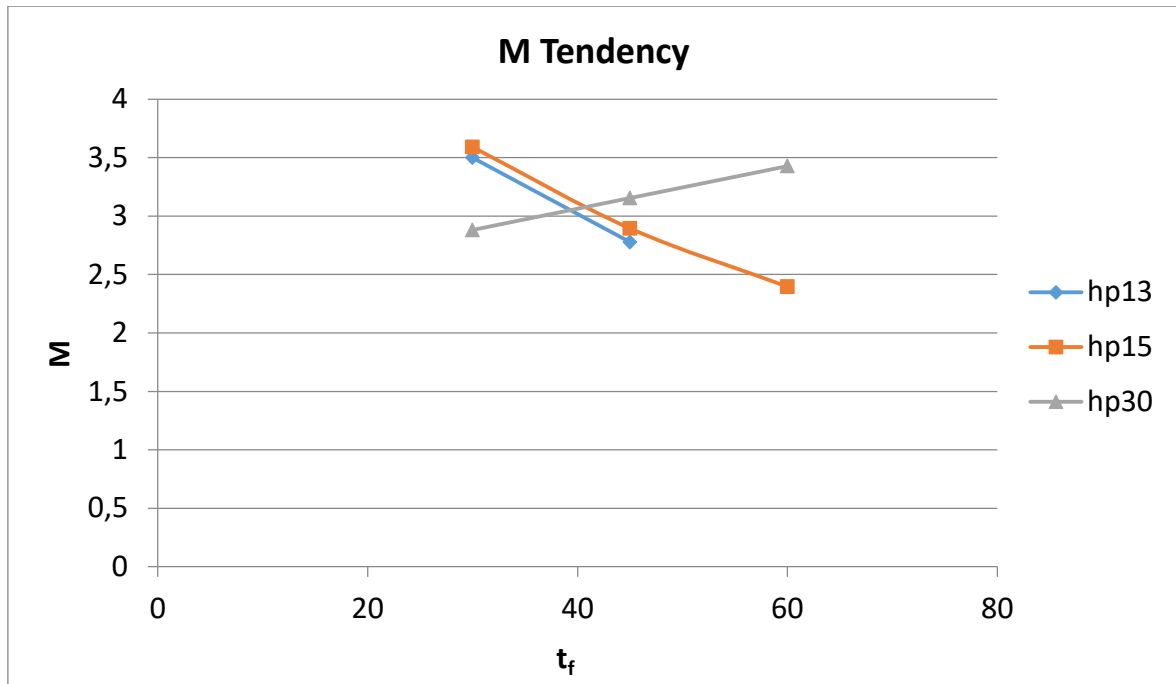
Firstly the data have to be analysed depending on those variables, the possible tendencies that they can have between them and the values obtained in the general equations, the ones shown in the *Table 8*.

General Equations (Corrected)		
$k_{3,1}=M*t^N$	M	N
h_p13t_f30	3,4990	-0,155
h_p13t_f45	2,7773	-0,139
h_p15t_f30	3,5900	-0,165
h_p15t_f45	2,8947	-0,112
h_p15t_f60	2,3963	-0,130
h_p20t_f30	2,8814	-0,118
h_p20t_f45	3,1543	-0,124
h_p20t_f60	3,4272	-0,106

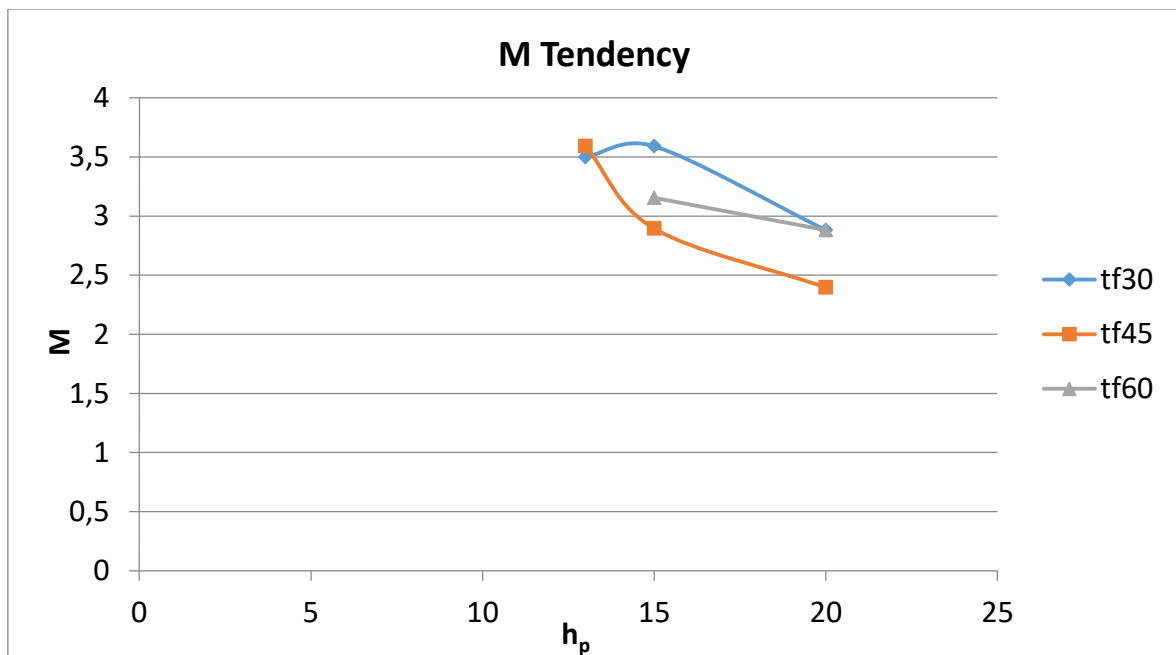
Table 8: General Equations Corrected

6.4.1 Parameter M

The first action is look for a tendency of the parameter M, which is the first one in the equation. For getting that put the parameter M is put in a graph depending on the values t_f and h_p as the *Graphs 13* and *14* shows.



Graph 13: M Tendency in function of t_f



Graph 14: M Tendency in function of h_p

It is best to find an equation that defines the curves of the M depending on each curve on the h_p and working in function of the variable t_f , which is the first option shown in the *Graph 13*. The The

The option 2 shown in the Graph 14 where the curve named by the t_f where the tendency depends directly on h_p is not used because they do not have any logic.

The curves for each case in the Graph 13 are in shown in the *Table 9* founded with lineal regressions.

M= A·t_f+B	Equation
h_p13	M= -0,0568·t _f +5,3342
h_p15	M= -0,053·t _f +5,4751
h_p20	M= 0,0182·t _f +2,3356

Table 9: General Equation for each h_p

The first two lines are very close and very similar so the parameters A and B must be very similar, but not the same. On the other hand the last case is very different as the other ones so the parameters A and B must be very different. All the calculations for getting these parameters are shown in the Appendix A. After the calculations the equation obtained for the parameter A and B are the following ones:

$$A = -0,055 + 0,073 \cdot e^{(h_p-20)}$$

$$B = 6,3 - 0,07 \cdot h_p - 2,7e^{(h_p-20)}$$

The equation for the parameter M of the General Equation is obtained if all the parts are joined:

$$M = \left(-0,055 + 0,073 \cdot e^{(h_p-20)} \right) \cdot t_f + 6,3 - 0,07 \cdot h_p - 2,7e^{(h_p-20)}$$

At the end the difference obtained by the parameter M are in the *Table 10*.

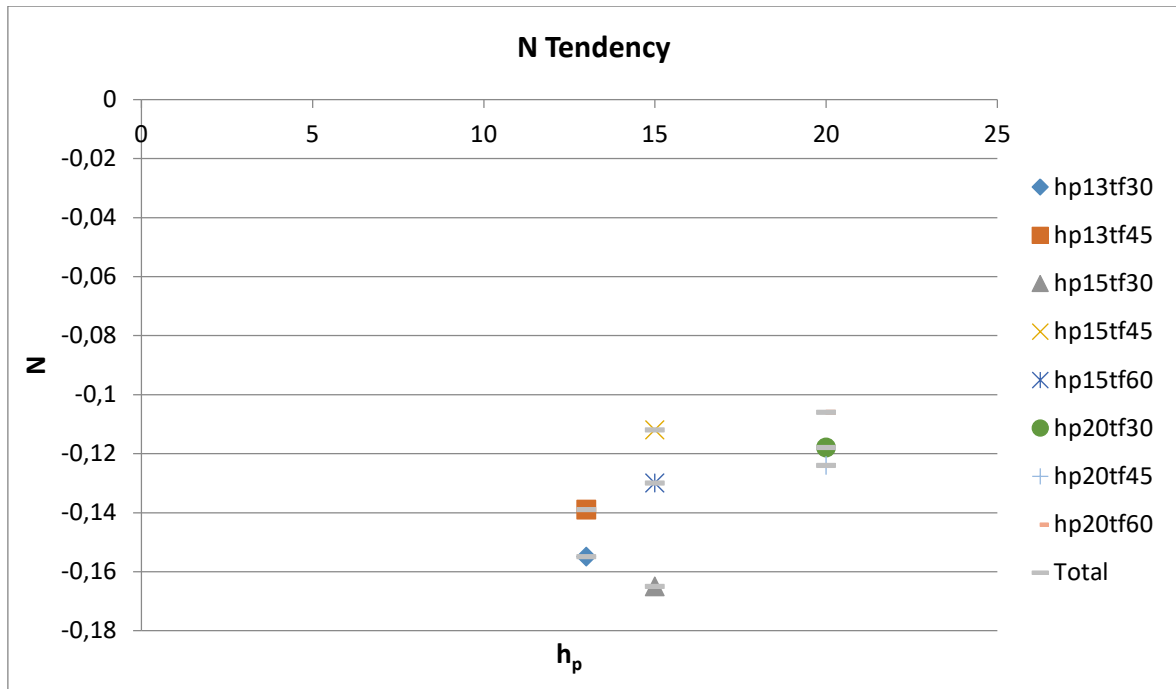
	hp	tf	M	A	A'	Difference	B	B'	Difference	M	M'	Difference
h_p13t_f30	13	30	3,499	-0,057	-0,055	3,29%	5,334	5,388	1,00%	3,4990	4,0895	16,88%
h_p13t_f45	13	45	2,777	-0,057	-0,055	3,29%	5,334	5,388	1,00%	2,7773	3,2155	15,78%
h_p15t_f30	15	30	3,590	-0,053	-0,055	2,85%	5,475	5,232	4,44%	3,5900	3,8966	8,54%
h_p15t_f45	15	45	2,895	-0,053	-0,055	2,85%	5,475	5,232	4,44%	2,8947	3,0789	6,36%
h_p15t_f60	15	60	2,396	-0,053	-0,055	2,85%	5,475	5,232	4,44%	2,3963	2,2613	5,63%
h_p20t_f30	20	30	2,881	0,018	0,018	1,10%	2,336	2,200	5,81%	2,8814	3,0400	5,50%
h_p20t_f45	20	45	3,154	0,018	0,018	1,10%	2,336	2,200	5,81%	3,1543	3,3100	4,94%
h_p20t_f60	20	60	3,427	0,018	0,018	1,10%	2,336	2,200	5,81%	3,4272	3,5800	4,46%
				Average		2%	Average		4%	Average		8,51%

Table 10: A, B, M parameters comparison and differences

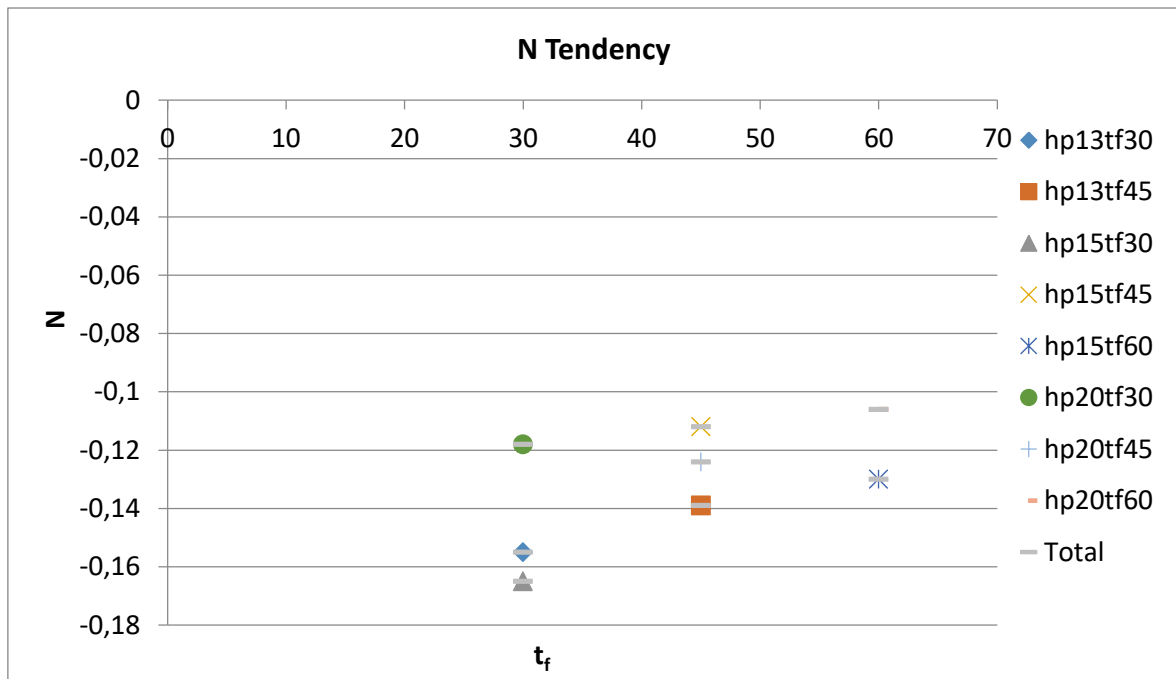
As the Table 10 shows the difference is lower than the 17% in all the cases. There is no need to worry about whether the difference regarding the M parameter wanted to obtain is very large because the important thing in the end is that the $k_{3,1}$ parameter obtained from the equation that seeks is greater than that obtained from the general equation. In this way the same parameter acts as a safety factor.

6.4.2 Parameter N

In this case the same procedure is followed with respect to the parameter M, with the objective of finding a trend of the parameter N respect one of the variables of time t, thickness of the protection board h_p and time of fall of the protection board t_f . The parameter N is shown depending on those variables in a graph for look for a tendency. The representation of the values that the parameter gives respecting the variables t_f and h_p are shown in the *Graphs 15* and *16*.



Graph 15 : N Tendency in function of h_p



Graph 16 : N Tendency in function of t_f

Here it is decided to divide the data into individual points because there was no coherent linearization between them based on h_p and t_f . The Graph 16 where the N values depend on the t_f variable has more linearity than in the graph where the N value depends on the h_p . For this reason

the *Graph 16* is chosen to find an equation that represents the N parameter with more accuracy. So the equation obtained from the *Graph 16* with a lineal regression shown below.

$$N = 0,001 * t_f - 0,1729$$

In this case is not necessary to look for the parameters of the equation because the parameter N does not affect much the final result of $k_{3,1}$ and the difference generated by N is not significantly affect the final result. Now the N' obtained from the equation and its differences are shown in the *Table 11*.

Size	hp	tf	N	N'	Difference
h_p13t_f30	13	30	-0,155	-0,14	9,68%
h_p13t_f45	13	45	-0,139	-0,125	10,07%
h_p15t_f30	15	30	-0,165	-0,14	15,15%
h_p15t_f45	15	45	-0,112	-0,125	11,61%
h_p15t_f60	15	60	-0,13	-0,11	15,38%
h_p20t_f30	20	30	-0,118	-0,14	18,64%
h_p20t_f45	20	45	-0,124	-0,125	0,81%
h_p20t_f60	20	60	-0,106	-0,11	3,77%
				Average	10,64%

Table 11: N parameters comparison and differences

6.4.3 Final equation

Once all the parameters obtained it is possible to find the final formula which show the coefficient $k_{3,1}$ depending on the variables on t_f and h_p for all the cases. And the final formula with all the parameters found is the *Formula 10*.

$$k_{3,1} = M \cdot t^N$$

$$k_{3,1} = (A \cdot t_f + B) \cdot t^N$$

Formula 10 : Base formula for $k_{3,1}$ developed

If all the parameters are substituted in the base equation shown in *Formula 9* the Final Formula we are looking for is obtained.

$$k_{3,1} = \left((-0,055 + 0,073 \cdot e^{(h_p-20)}) \cdot t_f + 6,3 - 0,07 \cdot h_p - 2,7 \cdot e^{(h_p-20)} \right) \cdot t^{(0,001 \cdot t_f - 0,17)}$$

And the simplification is:

$$k_{3,1} = \left(6,3 - 0,055 \cdot t_f - 0,07 \cdot h_p + (0,073 \cdot t_f - 2,7) \cdot e^{(h_p-20)} \right) \cdot t^{(0,001 \cdot t_f - 0,17)}$$

Formula 11: Final Formula for coefficient $k_{3,1}$

The simplification of the Final Formula is not very significant but that's because its structure does not allow it. Even so, it is clearer in the simplification therefore is left as definitive.

7 RESULTS AND ANALYSIS

Once the Final Formula is obtained, is need to know what degree of reliability this formula has for each specific case and to have in mind a general assessment of what consequences this difference may have. To have a complete vision each one of the $k_{3,1}$ is calculated with the formula and it is compared with the $k_{3,1}$ obtained with the simulation of the Safir program. Then with these two results the difference that exists in both is calculated. Showing all the results is very complicated since the information is very broad, that is why it is chosen to obtain the average difference for each case, and also show the maximum and minimum difference. Is necessary to remember that the equation gives an approximation of the values, not exactly the values, for this reason the difference could be bigger. The difference data is shown in the *Table 12*.

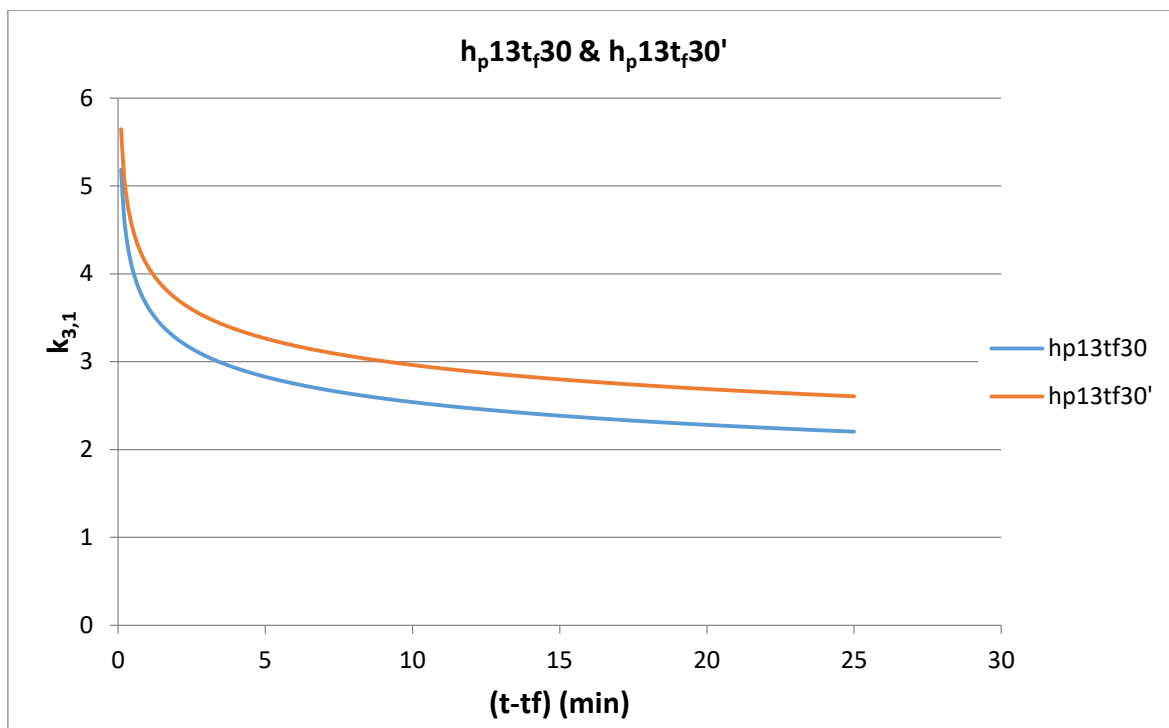
Difference			
Size	Difference _{Average}	Difference _{MAX}	Difference _{min}
hp13tf30	-17,25%	-18,47%	-11,43%
hp13tf45	-6,79%	-20,11%	-3,67%
hp15tf30	-12,85%	-2,41%	-14,99%
hp15tf45	-3,21%	-8,76%	-1,97%
hp15tf60	1,36%	10,96%	-0,64%
hpF20tf30	-0,42%	-9,90%	1,74%
hp20tf45	-4,49%	-4,92%	-4,40%
hp20tf60	-3,41%	-5,15%	-3,03%
Average	-5,88%	-7,34%	-4,80%

Table 12 : Difference averages, maximum and minimum for each size

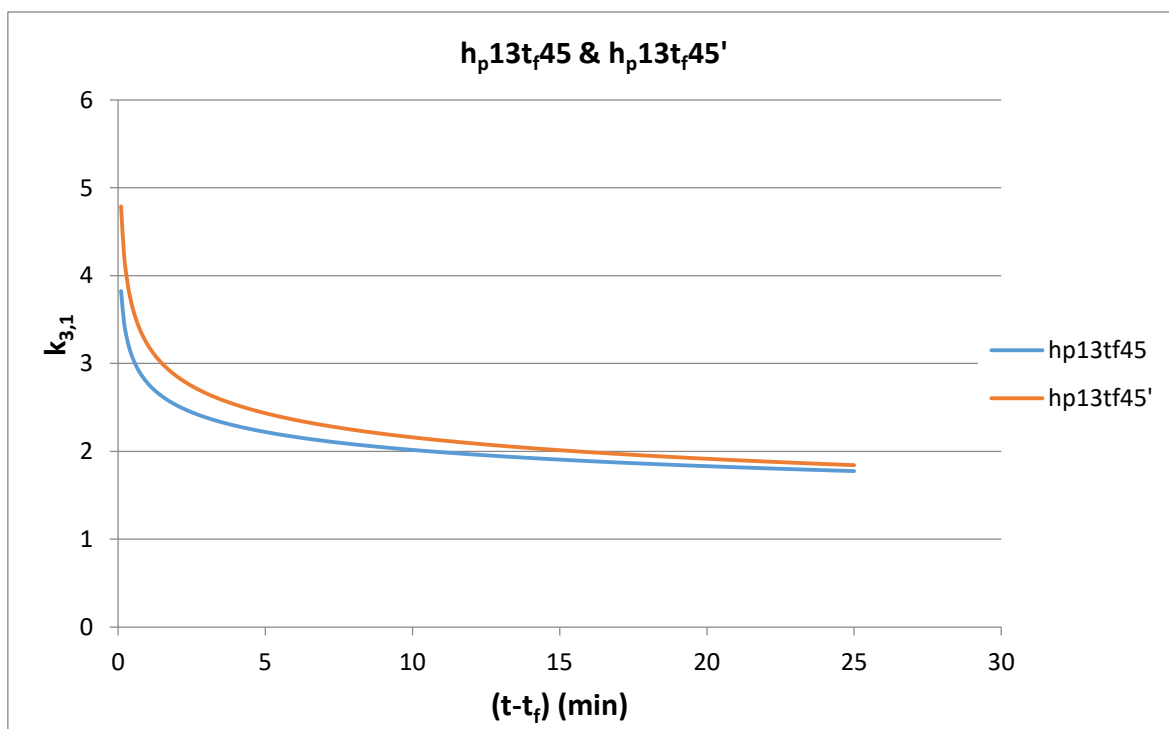
The maximum differences are around 10 -15% and even exceed 20%. This is not a problem because the difference in these cases happens because the coefficient $k_{3,1}$ is greater than that found with the Safir program, that is, the real value. The coefficient found with the formula to be greater acts as a safety coefficient, since to give higher values, always tend to oversize a little in this case the timber structures. To better understand how this formula works and the difference it gives, the graphs given have been compared with the Safir program information and the given with the formula with all the cases, which are shown below in the *Graphs 17,18,19,20,21,22,23* and *24*.

Where:

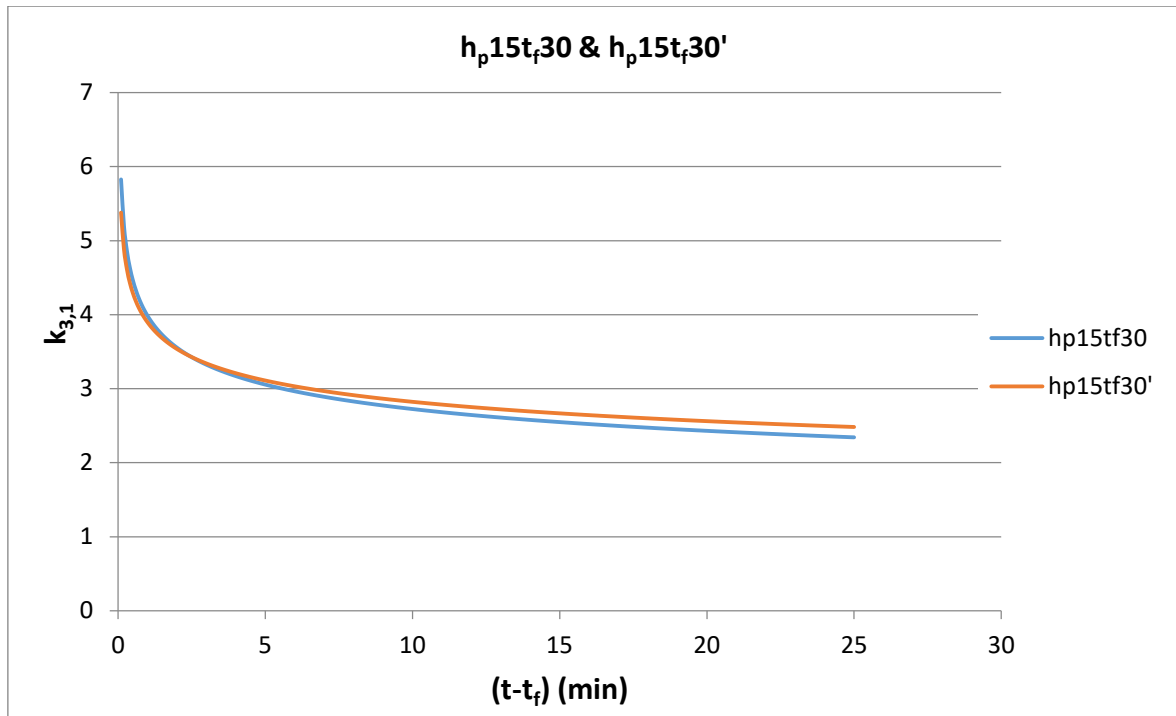
$$h_p t_f = \text{Safir data} \quad \& \quad h_p t_f' = \text{"Final Equation" data}$$



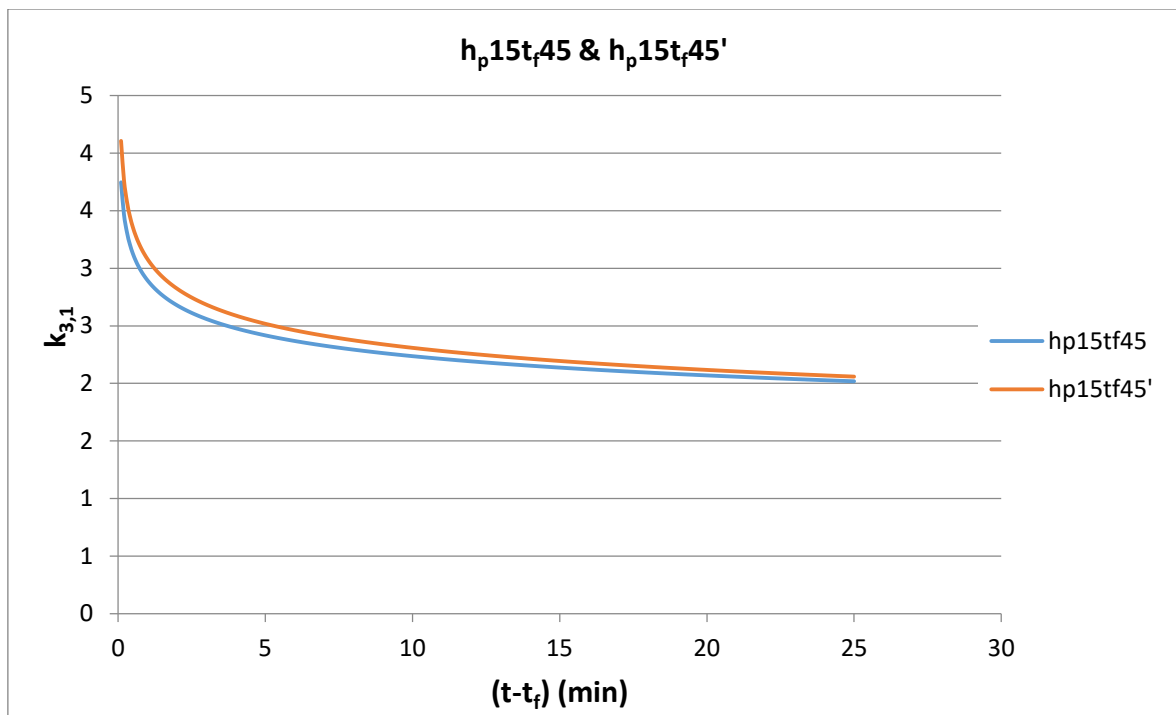
Graph 17: Comparison of h_{p13t_f30} & h_{p13t_f30}'



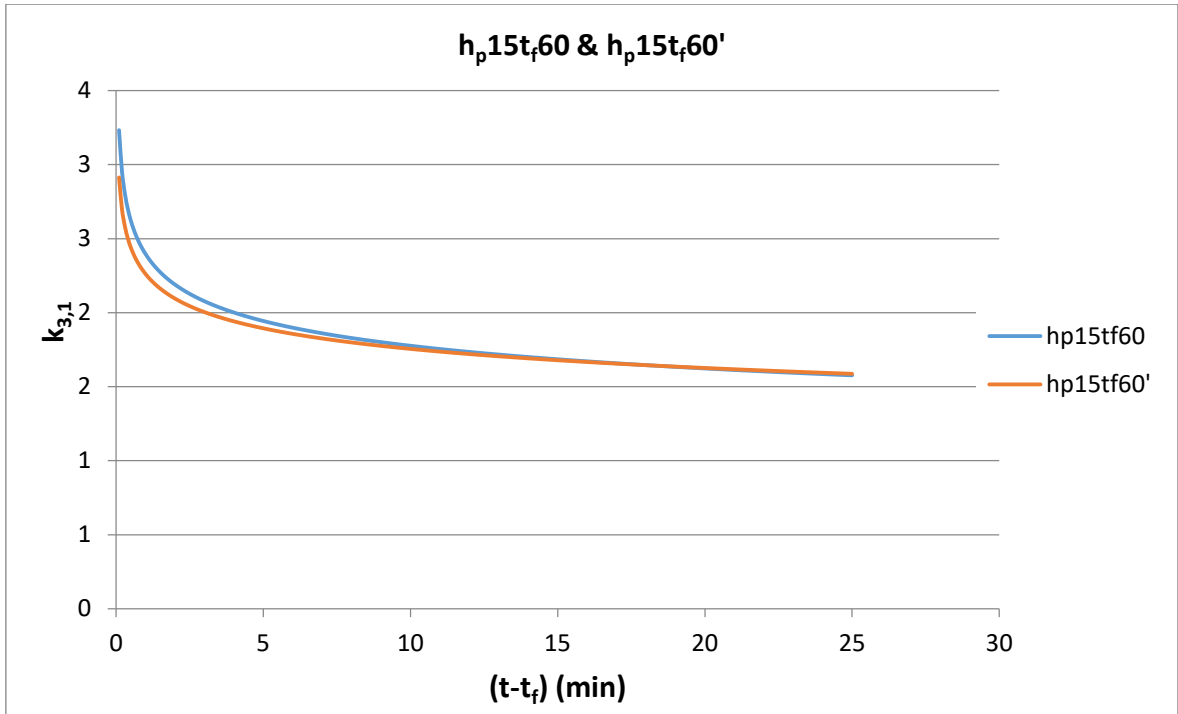
Graph 18: Comparison of h_{p13t_f45} & h_{p13t_f45}'



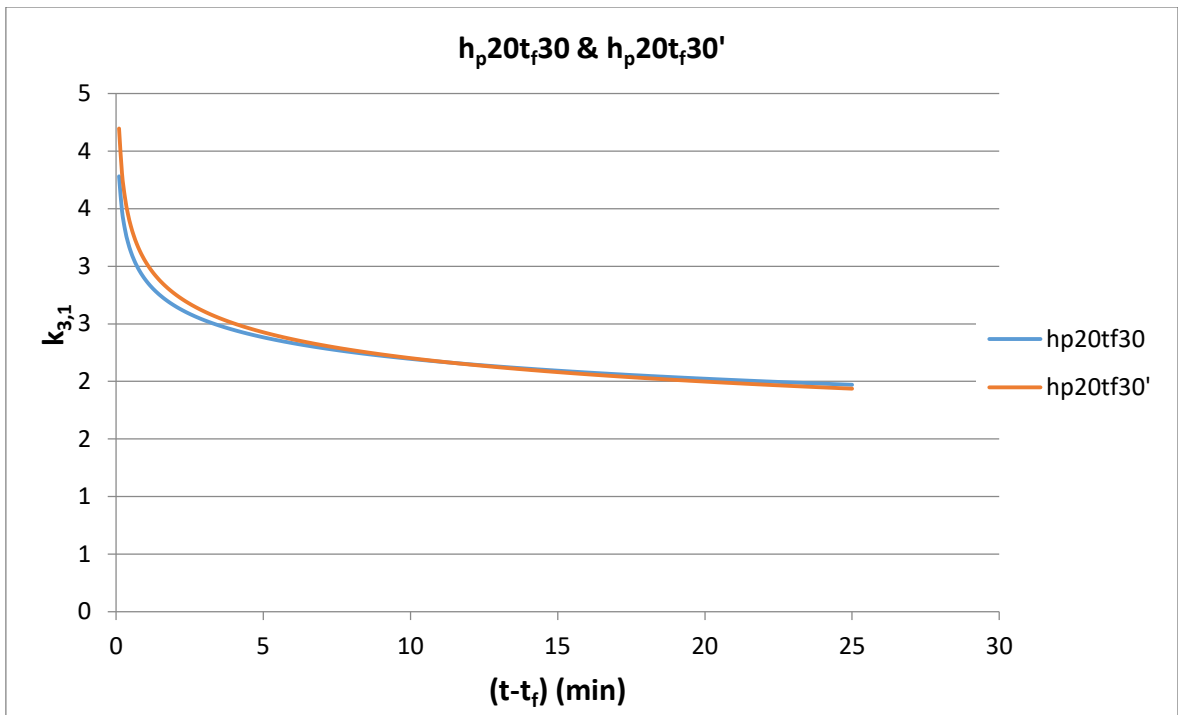
Graph 19: Comparison of h_{p15t_f30} & $h_{p15t_f30'}$



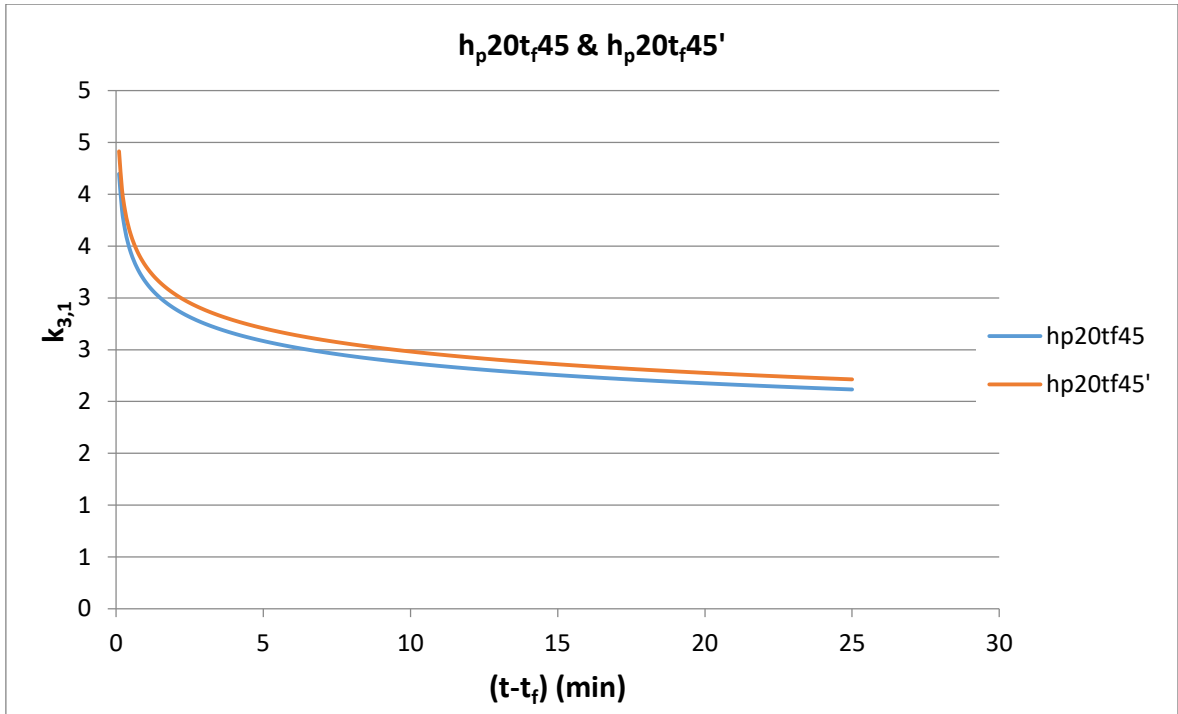
Graph 20: Comparison of h_{p15t_f45} & $h_{p15t_f45'}$



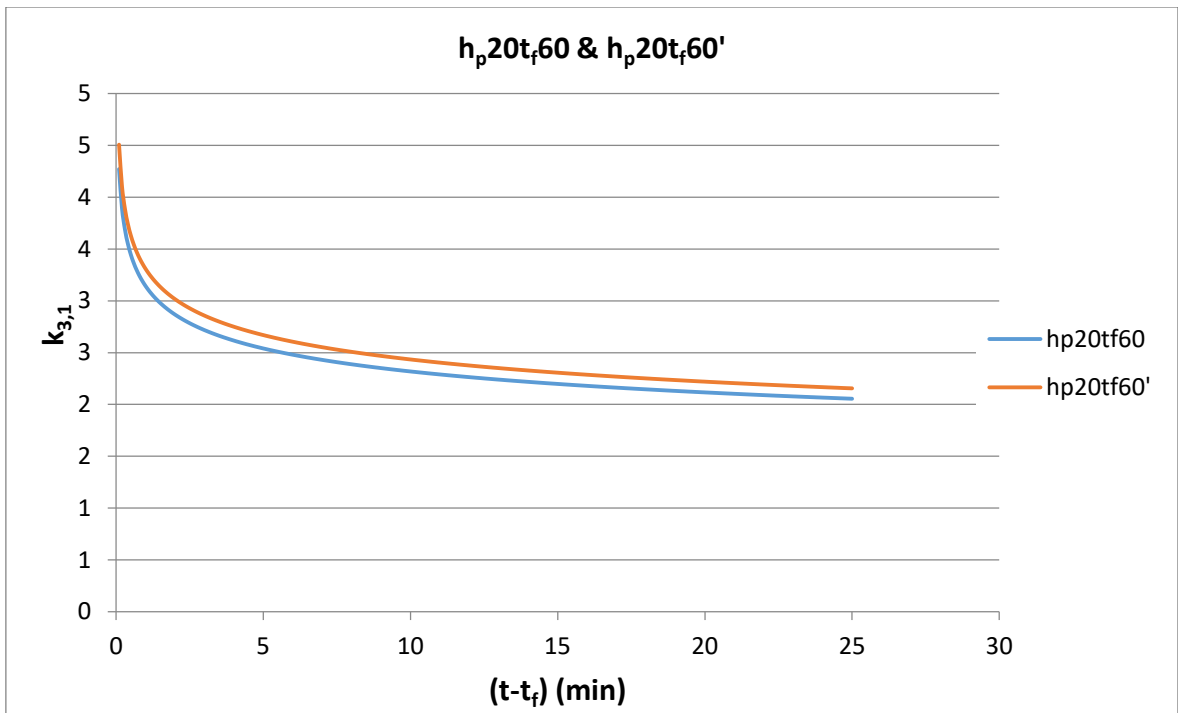
Graph 21: Comparison of h_{p15t_f60} & $h_{p15t_f60'}$



Graph 22: Comparison of h_{p20t_f30} & $h_{p20t_f30'}$



Graph 23: Comparison of h_{p20t_f45} & h_{p20t_f45}'



Graph 24: Comparison of h_{p20t_f60} & h_{p20t_f60}'

In almost all cases the values of the graph of the final equation are greater than the graph obtained from the Safir Program. In the cases where this rule is not met, the difference that is obtained is very small and can be taken as valid, since the difference it gives is not a serious problem as far as security is concerned. The maximum difference that is below the Safir data is 10% and at the beginning of the graph, when the carbonization layer has not yet been generated, at which time the values of $k_{3,1}$ are higher and an difference of 10% can be considered very low . All other differences are considered safety factors.

8 REAL TESTS COMPARISONS

Once all the study of the formula have been made, is need to know, to reliable results, whether this coefficient based on a simulation program sticks to reality. A comparison is made between the results that the formula gives and the results of the tests done in Bergen in the laboratory. In this laboratory a test was carried out with real I-joists in test furnaces where fire cases are simulated.

A difference of the simulation with Safir, the tests have only been done with 3 types of profiles: H200b47h47, HI200b70h47 and LVL200b47h39 and for each case a different insulation and a different type of beam are used which are shown in the Table 13.

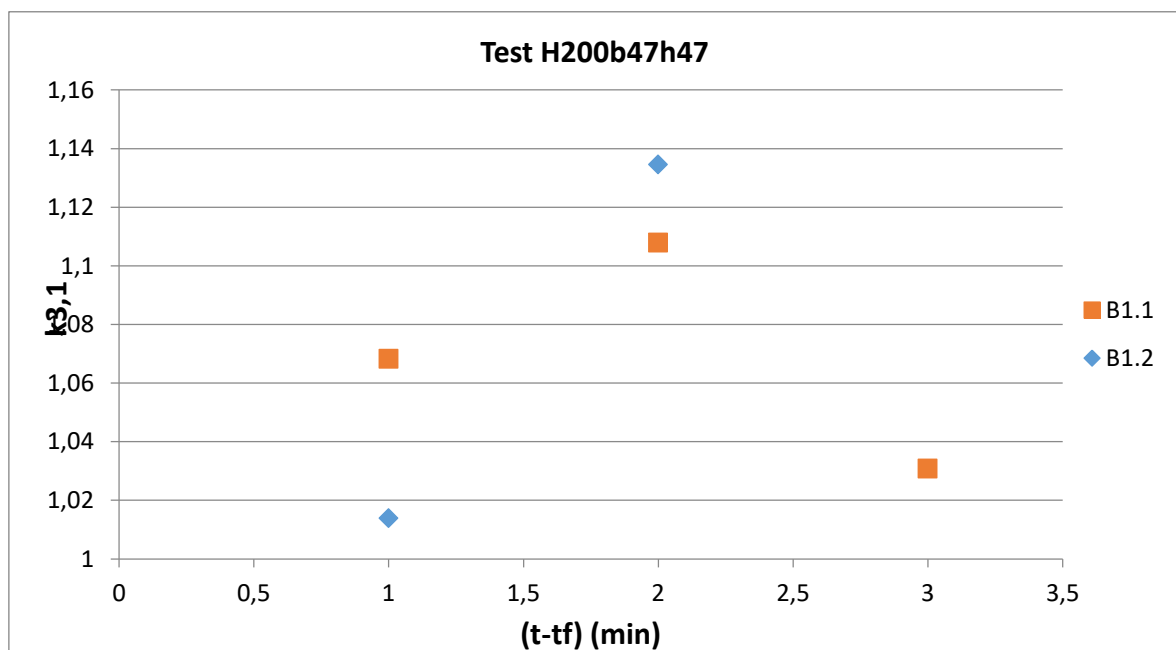
Beam	Case	Size	Web Insulation	Cavity Insulation
H200	B1.1	47x47	Expanded Polystyrene (EPS)	Stone Wool (SW)
H200	B1.2	47x47	Stone Wool (SW)	Stone Wool (SW)
H200	B1.3	47x47	Expanded Polystyrene (EPS)	Void
H200	B1.4	47x47	Glass Wool (GW)	Glass Wool (GW)
HI200	B2.1	70x47	Expanded Polystyrene (EPS)	Stone Wool (SW)
HI200	B2.2	70x47	Stone Wool (SW)	Stone Wool (SW)
HI200	B2.3	70x47	Expanded Polystyrene (EPS)	Void
HI200	B2.4	70x47	Glass Wool (GW)	Glass Wool (GW)
LVL200	B3.1	47x39	Expanded Polystyrene (EPS)	Stone Wool (SW)
LVL200	B3.2	47x39	Stone Wool (SW)	Stone Wool (SW)
LVL200	B3.3	47x39	Expanded Polystyrene (EPS)	Void
LVL200	B3.4	47x39	Glass Wool (GW)	Glass Wool (GW)

Table 13: Name of all cases

Only the results with the cases B1.1 and B1.2 are used because they have the stone wool insulation, which is used in the Safir simulations and the beam used is the H, the same as the one used in the Safir simulations. The comparison is not exact but it is possible to have an idea of what the trend of this parameter is in a real scenario. First of all the $k_{3,1}$ coefficient is calculated from all of this tests and they are compared with the rest of coefficients calculated in the simulations. From all the results take care only about the data after the fall of the protection board. The results obtained from those tests are the following ones shown in the *Table 14* and in the *Graph 25* for each case.

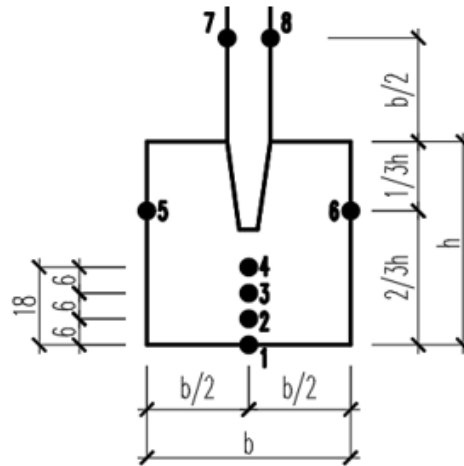
H200b47h47					
Thermocouple	d ₃₀₀ (mm)	t (min)	d _{char} (mm)	time (min)	K _{3,1}
Fall-off	5,8	26	0,0	0,0	-
B1.1 TC2	6	26,2	0,2	0,2	1,06831345
B1.1 TC3	12	31,4	6,2	5,4	1,107880615
B1.1 TC4	18	37,4	12,2	11,4	1,030828767
Fall-off	6,2	33	0,0	0,0	-
B1.2 TC3	12	38,5	5,8	5,8	0,961482105
B1.2 TC4	18	43,0	11,8	11,8	0,961482105

Table 14 : $k_{3,1}$ H200b47h47 Real Test



Graph 25: $k_{3,1}$ H200b47h47 Real Test

The tests have been done by placing three sensors on the flange which measure the temperature of the flange during the fire and tell us if it is being carbonized or not, as indicated in the *Picture 17*. The problem with these tests is that they only give 4 points to look at, different from the simulation that gives tens or hundreds of data. Therefore there are few points to compare, which directly affect the reliability of the comparison.



Picture 17 : Thermocouple Location

8.1 Comparisons

In each case the protection board has a 15,4 mm of thickness, so the comparisons must be done with the simulation cases where the h_p has a 15 mm of thickness. On the other hand the result the fall-off of the board is between 26 and 33 minutes and the average is around 30 minutes as the *Table 15* shows. So, all the cases are compared with the h_{p15t30} , because all its variables are the most similar with the real tests done.

Fall-off Time	
Case	Time (min)
B1.1	26
B1.2	33
B2.1	26
B2.2	33
B3.1	26
B3.2	33
Average	29,5

Table 15 : Fall-off Times

The comparison is done with the d_{char} , the $k_{3,1}$ at the same minutes as the thermocouples location are charred. This comparison shows if the simulation and the equation is reliable and gives a security factor enough for the d_{char} calculations in the future. And the comparisons are shown in the *Table 16*.

I-joist case	Time (min)	H200b47h47 Results						
		Real Tests		Safir Simulation		Equation	Difference	
		dchar' (mm)	$k_{3,1}$	dchar' (mm)	$k_{3,1}$	$k_{3,1}$	Real Test	Error Safir
B1.1	0	0,0	-	-	-	-	-	-
	0,2	0,2	1,07	1	5,72	4,88	-78%	-15%
	5,4	6,2	1,11	12	2,11	3,08	-64%	46%
	11,4	12,2	1,03	22	1,84	2,77	-63%	51%
B1.2	0	0,0	-	-	-	-	-	-
	5,5	5,8	1,01	12,0	2,08	3,07	-67%	48%
	10	11,8	1,13	20	1,91	2,82	-60%	48%

Table 16 : $k_{3,1}$ Comparison with real, Safir and Equation results

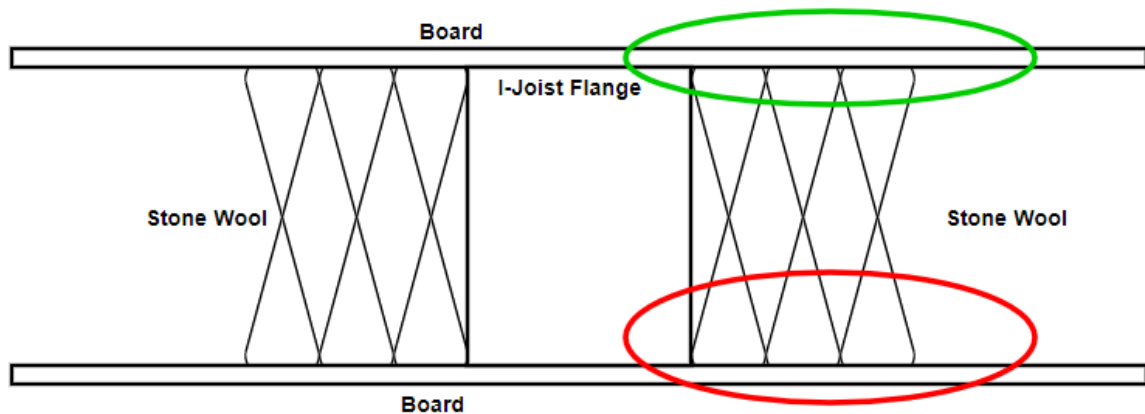
In the Table 16 the difference obtained from the Real tests between the Safir data and the Equation Data are bigger than expected. It is explained in the following chapter why this phenomenon could happen.

9 CONCLUSIONS

As the *Table 15* shows, the difference of the data of the simulations with Safir and those obtained with the formula are considerably large, with a difference higher than expected. With the actual tests coefficient $k_{3,1}$ tends to 1 while in Safir and in Final Equation the difference tends to stabilize only once a considerable time between 2.5 and 1.5 has elapsed. That difference can occur for different reasons, which are explained below.

9.1 Safir Imprecisions

The Safir program works by means of information introduced regarding the structure and information introduced regarding the fire and the temperatures that it usually reaches. The Safir program can tell with exact precision the temperatures reached in the upper part of the structure, in the green part of the *Picture 18*. But on the other hand it has many difficulties to tell precisely what the real temperatures are to the bottom of the structure, the red part indicated in *Picture 18*.



Picture 18: Timber structure with stone wool insulation and protection board

This problem could happen because the isolation of stone wool is a complicated material to define in Safir and if the coefficients that define how the fire behaves with this material are not correctly introduced, it can give erroneous results. For this reason, the Safir program may give different results in the studied area where carbonization occurs. According to the results of the

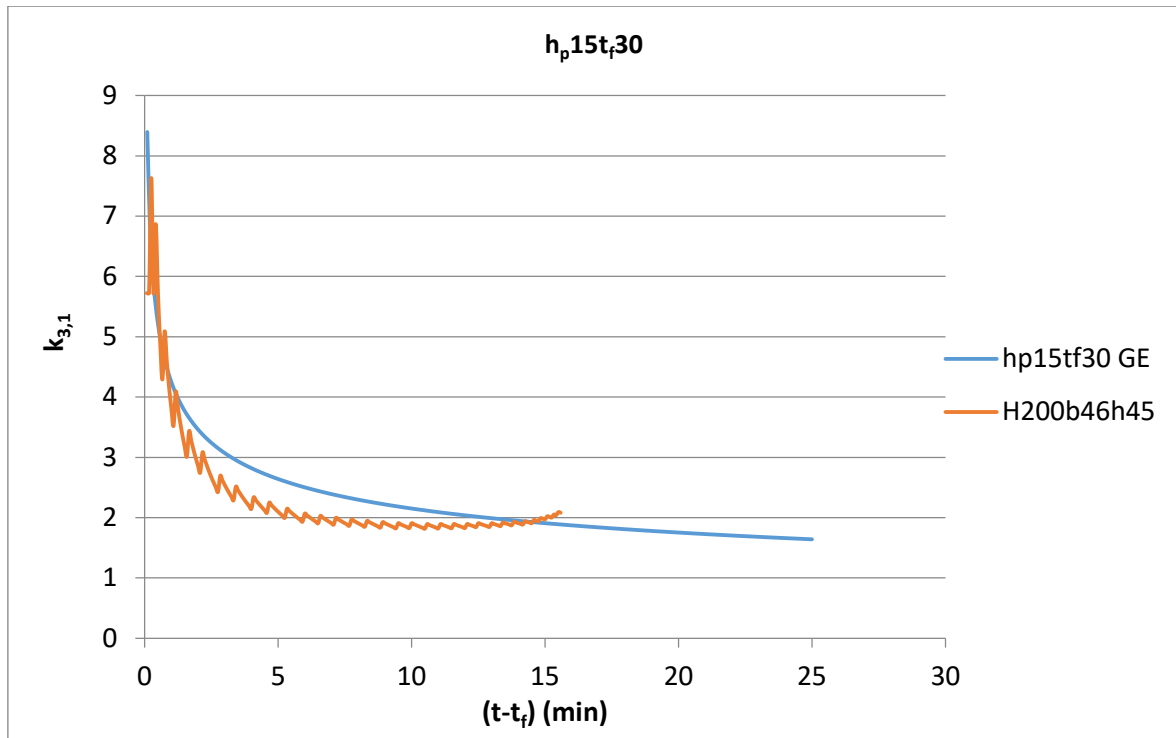
real tests the $k_{3,1}$ and d_{char} should be lower. Therefore, the Safir program tells that timber burns more quickly than it actually does and therefore, this leads to larger coefficients of majorization.

A solution for this type of problem would be to correct and calibrate the coefficients that define the fire in stone wool according to how it acts in real cases. For that more data of real cases must be obtained because with the current ones in this study it is impossible to make a calibration with the adequate accuracy. On the other hand, if you wanted to make a correction of the Final Equation, is possible to add a minimizing coefficient that brings the results obtained to match the actual cases obtained.

By having a formula that defines the trend of the coefficient $k_{3,1}$ in a very precise way according to the Safir Program data, with a correction of the parameters that define the simulation of the Safir Program, a correction of the formula could be made so that it would give true values to reality. It would not be necessary to redo the entire procedure to obtain the final formula.

9.2 General Equation differences

Another reason why this difference can be given is the fact of comparing an equation that defines a multitude of cases with a single one in particular. The test has been done in an I-joist profile of H200b47h47, which is one of the smallest studied and which can give lower results than the general average. In the *Graph 26*, the difference between the values is quite large.



Graph 26 : Differences between General Equation and equation for the size H200b46h45

The difference between both cases at minute 2 and minute 10 is considerably large, so part of the difference may come out of here. But this would not be what would actually produce the difference because the data is taken from Safir and the equation is taken based on this data. So is possible to conclude that this factor would only affect casually and without a considerably important difference. Only the difference increases relatively.

10 SUMMARY

10.1 English Summary

In this study the behaviour of structural I-joist for infrastructures under the effects of fire it's been analysed. The study is based on the treatment of data on the carbonization of the structural elements and their progression depending on the proportions of the beam I, the time of fall and thickness of the protective board. The objective of this study was to define a Final Formula for the coefficient $k_{3,1}$ that defines the effects of fire on the I-joists once the protection board has fallen in case of fire.

First of all, data from a simulator called Safir have been obtained and these data have been processed and simplified using Matlab. Once the correct data has been obtained, we analysed it with the final objective of obtaining a Final Formula that defines the $k_{3,1}$ coefficient in a simple and simple way, which is shown below.

$$k_{3,1} = \left(6,3 - 0,055 \cdot t_f - 0,07 \cdot h_p + (0,073 \cdot t_f - 2,7) \cdot e^{(h_p - 20)} \right) \cdot t^{(0,001 \cdot t_f - 0,17)}$$

Once the Final Formula has been obtained, several comparisons have been made to verify that the results they give are correct. The first comparison was with the data obtained from Safir and the differences have been relatively small see in the following table shows:

Total Differences		
Difference _{Average}	Difference _{MAX}	Difference _{min}
-5,88%	-7,34%	-4,80%

The Final Formula represents correctly the values and tendencies obtained from the data of the Safir simulator, therefore it's possible to say that it is correct.

On the other hand we have also compared the results of the formula with the results obtained from the tests carried out in the laboratory. These results would be the most approximate information to the reality so the results are conclusive. In the following table we can see the

different results obtained by a specific profile used in the tests and the respective comparison with the data of Safir and the Final Formula:

I-joist case	H200b47h47 Results				
	$k_{3,1}$			Difference	
	Real Tests	Safir Simulation	Final Equation	Real Test	Safir Simulation
B1.1	-	-	-	-	-
	1,07	5,72	4,88	-78%	-15%
	1,11	2,11	3,08	-64%	46%
	1,03	1,84	2,77	-63%	51%
B1.2	-	-	-	-	-
	1,01	2,08	3,07	-67%	48%
	1,13	1,91	2,82	-60%	48%

The results are too different, so the formula has been adapted to the values obtained by the Safir simulator, but they don't coincide with the real cases.

From these data it's been concluded that Safir's data is not entirely correct. This is because when defining structure and isolation in the simulator the coefficients are not well entered and as a consequence the simulator correctly reads the temperatures at the top of the structure but not at the bottom where the carbonization is studied. On the other hand the fact of comparing only the results of a profile exaggerates the results since the Final Formula is based on the average of several curves and what is mainly done represents the tendency of each case studied.

As a solution, it could be proposed to adjust the variables that define the fire in the simulator and from this adjustment the Final Formula obtained could be modified so that it gives the results obtained from the real cases, in order to represent it more correctly as it has an I-joist in case of fire.

10.2 Resum en català

En aquest estudi s'ha analitzat el comportament de biguetes i estructurals per a infraestructures sota els efectes del foc. L'estudi s'ha basat en el tractament de dades sobre la carbonització dels elements estructurals i la seva progressió depenent de les proporcions de la bigueta i, el temps de caiguda i gruix de la placa de protecció. L'objectiu d'aquest estudi ha estat definir una equació per al coeficient $k_{3,1}$ que defineix els efectes del foc sobre les biguetes i un cop la placa de protecció ha caigut en cas d'incendi.

Primer de tot s'han obtingut dades d'un simulador anomenat Safir i seguidament s'han tractat i simplificat aquestes dades mitjançant el Matlab. Un cop obtingudes les dades correctes s'han analitzat amb l'objectiu final d'obtenir una fórmula que definís el coeficient $k_{3,1}$ d'una manera simple i senzilla, la qual es pot veure a continuació:

$$k_{3,1} = \left(6,3 - 0,055 \cdot t_f - 0,07 \cdot h_p + (0,073 \cdot t_f - 2,7) \cdot e^{(h_p - 20)} \right) \cdot t^{(0,001 \cdot t_f - 0,17)}$$

Un cop obtinguda la Fórmula Final s'han realitzat varies comparacions per a comprovar que els resultats que dona són correctes. La primera comparació ha estat amb les dades obtingudes a partir de Safir i les diferències han estat relativament petites tal i com es pot veure a la taula següent:

Diferències Totals		
Diferència _{Mitjana}	Diferència _{MAX}	Diferència _{min}
-5,88%	-7,34%	-4,80%

La Fórmula Final és fidel als valors i tendències obtingudes a partir de les dades del simulador Safir, per tant es pot dir que és correcta.

Per altra banda s'ha comparat també els resultats de la fórmula amb els resultats obtinguts dels tests realitzats al laboratori. Aquests resultats serien la informació més aproximada a la realitat per tant els resultats són concloents. A la taula següent es pot veure els diferents resultats obtinguts per un perfil concret utilitzat als tests i la respectiva comparació amb les dades de Safir i la Fórmula Final:

Cas de Bigueta I	H200b47h47 Resultats				
	$k_{3,1}$			Diferències	
	Tests Reals	Simulació Safir	Equació Final	Test Real	Simulació Safir
B1.1	-	-	-	-	-
	1,07	5,72	4,88	-78%	-15%
	1,11	2,11	3,08	-64%	46%
	1,03	1,84	2,77	-63%	51%
B1.2	-	-	-	-	-
	1,01	2,08	3,07	-67%	48%
	1,13	1,91	2,82	-60%	48%

Tal I com es pot veure els resultats son massa diferents per tant es podria dir que la formula s'ha adaptat als valors obtinguts pel simulador Safir però aquests dos últims no coincideixen amb els casos reals.

A partir d'aquestes dades s'ha conclòs que les dades de Safir no son del tot correctes. Això succeeix ja que al definir l'estructura i l'aïllament al simulador els coeficients no estan ben entrats i com a conseqüència el simulador llegeix correctament les temperatures a la part superior de l'estructura però no a la part inferior on hi estem estudiant la carbonització. Per altre banda el fet de comparar tan sols els resultats d'un perfil exagera els resultats ja que la Formula Final està basada en la mitjana de varies corbes i el que principalment fa es representar la tendència de cada cas estudiat.

Com a solució es podria proposar ajustar les variables que defineixen e foc al simulador i a partir d'aquest ajust es podria modificar la Fórmula Final obtinguda de manera que ens doni els resultats obtinguts dels casos reals, per tal de representar de manera més correcta com es comporta una bigueta en I en cas d'incendi.

11 LIST OF REFERENCES

- [1] “ÁREA TÉCNICA-AITIM-MADERA PROTECCIÓN DE LA MADERA-Estructuras madera y fuego- Fecha COMPORTAMIENTO AL FUEGO DE LAS ESTRUCTURAS DE MADERA.”
- [2] “Evolución de la construcción con madera – Maderas Besteiro.” [Online]. Available: <https://mbesteiro.com/blog/evolucion-de-la-construccion-con-madera/>. [Accessed: 26-Feb-2019].
- [3] “Breve historia de la madera como material de construcción - Madera.” [Online]. Available: <http://www.interempresas.net/Madera/Articulos/44265-Breve-historia-de-la-madera-como-material-de-construccion.html>. [Accessed: 26-Feb-2019].
- [4] “Vivienda: El 18% de la población mundial vive en casas construidas en madera | EL MUNDO.” [Online]. Available: <https://www.elmundo.es/economia/2014/06/23/53a8151f22601de27f8b4580.html>. [Accessed: 11-Apr-2019].
- [5] “Casas de madera: ventajas e inconvenientes.” [Online]. Available: <https://www.ecologiaverde.com/casas-de-madera-ventajas-e-inconvenientes-435.html>. [Accessed: 27-Feb-2019].
- [6] “Ventajas e inconvenientes de las casas de madera prefabricadas baratas.” [Online]. Available: https://hogar.uncomo.com/articulo/ventajas-e-inconvenientes-de-las-casas-de-madera-prefabricadas-baratas-47100.html#anchor_3/. [Accessed: 25-Feb-2019].
- [7] “El estudio del fuego en estructuras de maderas | Maderea.” [Online]. Available: <https://www.maderea.es/el-estudio-del-fuego-en-estructuras-de-maderas/>. [Accessed: 15-Mar-2019].
- [8] Structural Timber Association, “Fire safety in timber buildings,” 2013.
- [9] “EN 1995-1-2: Eurocode 5: Design of timber structures - Part 1-2: General - Structural fire design.”
- [10] Katrin Nele Mäger, *Parameters and tests for the design model for I-joists in fire*. .
- [11] E. Allen and P. Rand, *Architectural detailing : function, constructibility, aesthetics*. .

- [12] Eck, Curtis. "Wood I-Joist Do's and Don'ts." *Journal of Light Construction* (Sept. 1995) - Cerca amb Google. .
- [13] Vogt, Floyd. *Carpentry. 4th ed.* Clifton Park, NY: Thompson Delmar Learning, 2001 - Cerca amb Google. .
- [14] "Report on Structural Stability of Engineered Lumber in Fire Conditions," Sep. 2008.
- [15] A. Earls, "Lightweight Construction," 2009.
- [16] J.-M. Franssen and T. Gernay, "Modeling structures in fire with SAFIR[®] : theoretical background and capabilities," *Journal of Structural Fire Engineering*, 11-Sep-2017. [Online]. Available: <http://www.emeraldinsight.com/doi/10.1108/JSFE-07-2016-0010>. [Accessed: 01-Apr-2019].

12 Appendix A : Calculations for the equation

The type of equation has a potential shape, and its structure is shown in the *Formula A1*.

$$y = M \cdot x^N$$

Formula A1: Base formula for $k_{3,1}$

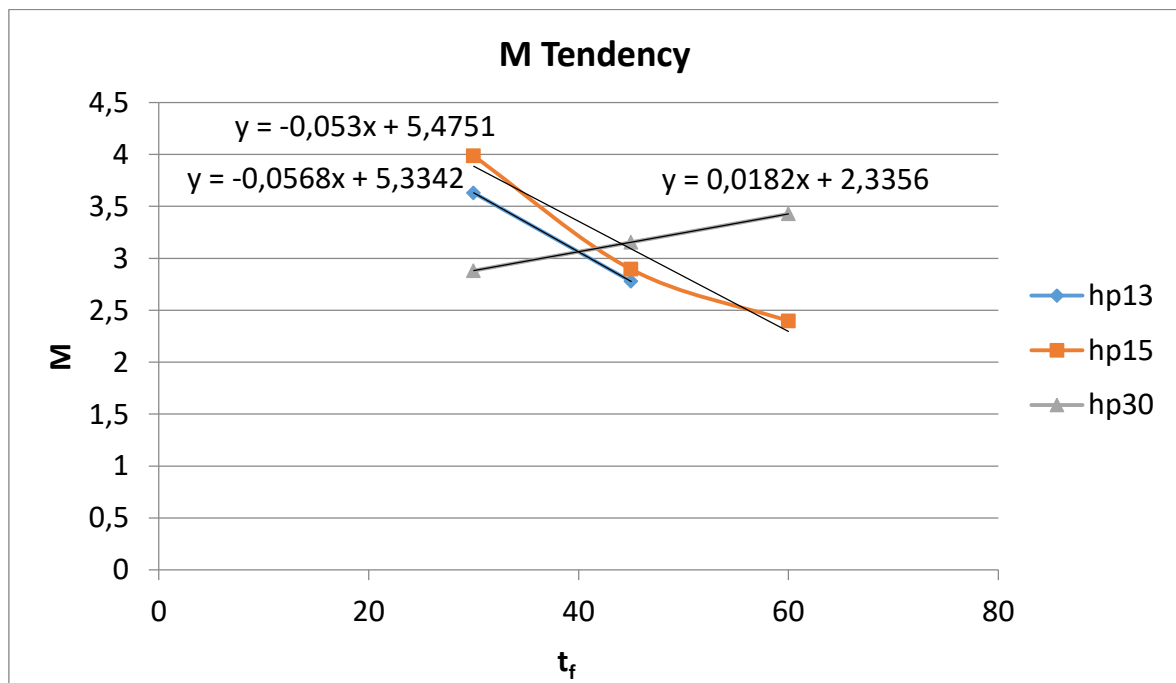
Where:

$$y = k_{3,1}$$

$$x = \text{time "t"}$$

12.1 Parameter M

First of all is necessary to know that the calculation of the formula is obtained going in parts. First of all, the equations from the *Graph A1* chosen for getting the M parameter are analysed.



Graph A1: M Tendency graph

The equations obtained from it are the following ones:

$$M = -0,0568 \cdot t_f + 5,3342$$

$$M = -0,053 \cdot t_f + 5,4751$$

$$M = 0,0182 \cdot t_f + 2,3356$$

So the parameter M equation must have this shape:

$M = A \cdot t_f + B$

Formula A2: Base formula for M

Both of the first equations are very similar each other, so firstly I put the base of the equation in the average of the parameters of this two equations.

$$A_{Average} = \frac{-0,0568 - 0,053}{2} = -0,0549$$

$$B_{Average} = \frac{5,3342 - 5,4751}{2} = 5,4047$$

So the Average Equation I get is:

$$k_{3,1} = -0,0549 \cdot t_f + 5,4047$$

Once I have the base of the equation is necessary to have the differences between the parameters A and B of both equations with the average equation, which are the following ones:

$$A = -0,0549 \pm 0,0019$$

$$B = -5,409 \pm 0,0661$$

Now is necessary that an equation gives those values depending on the case using one of the variables. In this it is decided to use the h_p variable to get it, and the result is the following one:

$$A_{12} = -0,0549 - 0,0019 \cdot (h_p - 14)$$

$$B_{12} = 5,409 - 0,0661(h_p - 14)$$

Now the base of this equation is used for getting the parameters of the equation three, which is really different between the others. The differences between the equation base and the equation 3 are:

$$A_3 = A_{12} + 0,0731$$

$$B_3 = B_{12} - 3,734$$

Here we need a part of the equation that has an important value from a number but when this number is smaller the part of the equation has to be negligible. It is decided to use the constant e raised to a potential that varies with respect to h_p , because this variable is what differentiates this equation from the others. I only need this number be a 1 for one number and then for a lower number have a very low value, and I took this way:

$$e^{h_p-20}(h_p = 13) = 9,11 \cdot 10^{-4}$$

$$e^{h_p-20}(h_p = 15) = 6,74 \cdot 10^{-4}$$

$$e^{h_p-20}(h_p = 20) = 1$$

I then a number that multiplied by this part give the difference between the base equation and the parameters A_3 and B_3 . And the formula obtained for each parameter is the following one:

$$A_3 = A_{12} + 0,0731 \cdot e^{h_p-20}$$

$$B_3 = B_{12} - 3,734 \cdot e^{h_p-20}$$

So at the end the two parameters are:

$$A_3 = -0,0549 - 0,0019 \cdot (h_p - 14) + 0,0731 \cdot e^{h_p-20}$$

$$B_3 = 5,409 - 0,0661(h_p - 14) - 3,734 \cdot e^{h_p-20}$$

And all the M parameter is:

$$M = A \cdot t_f + B$$

$$M = (-0,0549 - 0,0019 \cdot (h_p - 14) + 0,0731 \cdot e^{h_p-20}) \cdot t_f + 5,41 - 0,0661(h_p - 14) - 3,734 \cdot e^{h_p-20}$$

Once the formula is obtained, it is realized that the next part does not affect the result very much because the values it gives are very small and it is decided to eliminate it. Below is shown how little the results vary:

$$h_p = 13 \quad \rightarrow \quad -0,0019 \cdot (h_p - 14) = 1,9 \cdot 10^{-3}$$

$$h_p = 15 \quad \rightarrow \quad -0,0019 \cdot (h_p - 14) = -1,9 \cdot 10^{-3}$$

$$h_p = 20 \quad \rightarrow \quad -0,0019 \cdot (h_p - 14) = -0,0114$$

This part of the equation is deleted, the formula became simpler and the results and differences are the same. So the formula of M is shown in the *Formula A3*.

$$M = (-0,0549 + 0,0731 \cdot e^{h_p-20}) \cdot t_f + 5,409 - 0,0661(h_p - 14) - 3,734 \cdot e^{h_p-20}$$

Formula A3: Base formula for M depending of h_p and t_f

Rounding the values, always watching that they do not affect the difference that the formula gives, we must ensure that it is in the form of a safety coefficient. The *Formula A4* shows the Final Formula.

$$M = (-0,055 + 0,073 \cdot e^{h_p-20}) \cdot t_f + 5,41 - 0,0661(h_p - 14) - 3,73 \cdot e^{h_p-20}$$

Formula A4 : Base formula for M depending of h_p and t_f simplified

13 Acknowledgments

First of all, I would like to thank Professor Alar Just and the future Doctor Katrin Nele Mäger for the Master Thesis that they have proposed and for all the help and support they have given me during this semester.

I also want to thank Taltech for having received me as a student and allowed me to do the Master Thesis in Tallinn.